The Journal of Comparative Neurology 516:291–311 (2009)
Research in Systems Neuroscience

Quantitative Analysis of Neurons with Kv3 Potassium Channel Subunits, Kv3.1b and Kv3.2, in Macaque Primary Visual Cortex

CHRISTINE M. CONSTANTINOPLE,[1] ANITA A. DISNEY,[1]* JONATHAN MAFFIE,[2] BERNARDO RUDY,[2] AND MICHAEL J. HAWKEN[1]
[1]Center for Neural Science, New York University, New York, New York 10003
[2]Smilow Neuroscience Program and Department of Physiology and Neuroscience, New York University School of Medicine, New York, New York 10016

ABSTRACT

Voltage-gated potassium channels that are composed of Kv3 subunits exhibit distinct electrophysiological properties: activation at more depolarized potentials than other voltage-gated K+ channels and fast kinetics. These channels have been shown to contribute to the high-frequency firing of fast-spiking (FS) GABAergic interneurons in the rat and mouse brain. In the rodent neocortex there are distinct patterns of expression for the Kv3.1b and Kv3.2 channel subunits and of coexpression of these subunits with neurochemical markers, such as the calcium-binding proteins parvalbumin (PV) and calbindin D-28K (CB). The distribution of Kv3 channels and interrelationship with calcium-binding protein expression has not been investigated in primate cortex. We used immunoperoxidase and immunofluorescent labeling and stereological counting techniques to characterize the laminar and cell-type distributions of Kv3-immunoreactive (ir) neurons in macaque V1. We found that across the cortical layers ≈25% of both Kv3.1b- and Kv3.2-ir neurons are non-GABAergic. In contrast, all Kv3-ir neurons in rodent cortex are GABAergic (Chow et al. [1999] J Neurosci. 19:9332–9345). The putatively excitatory Kv3-ir neurons were mostly located in layers 2, 3, and 4b. Further, the proportion of Kv3-ir neurons that express PV or CB also differs between macaque V1 and rodent cortex. These data indicate that, within the population of cortical neurons, a broader population of neurons, encompassing cells of a wider range of morphological classes may be capable of sustaining high-frequency firing in macaque V1. J. Comp. Neurol. 516:291–311, 2009.

Indexing terms: potassium channels; striate cortex; GABAergic; dual-labeling; immunofluorescence; calcium-binding proteins; parvalbumin; Meynert cells; spiny neurons; excitatory neurons

Mammalian neocortex shows a rich diversity of neuronal types. Determining the relationships between the classes of neurons in the cortical circuit is a key factor in understanding how the cortex works. One of the simplest ways to classify neocortical neurons is according to their primary neurotransmitter substance, which in the neocortex is either glutamate or γ-aminobutyric acid (GABA) for the vast majority of neurons (reviewed by DeFelipe, 1993). The subset of neocortical neurons that expresses the inhibitory transmitter GABA is very diverse and shows variation across species (DeFelipe, 1993; DeFelipe et al., 2002). A commonly used subclassification for this population is based on physiological properties and divides GABAergic neurons into "fast-spiking" (FS) and nonfast-spiking (non-FS) types. It has been well demonstrated in rodent neocortex that FS neurons can be identified anatomically by their expression of the calcium-binding protein parvalbumin (PV; Kawaguchi and Kubota, 1993; Cauli et al., 1997; Kawaguchi and Kubota, 1997; Toledo-Rodriguez et al., 2004). PV-immunoreactive (PV-ir) neurons comprise ≈50% of the inhibitory interneurons within the rodent neocortex (Gonchar and Burkhalter, 1997) and include cell types, mainly basket and chandelier, which provide powerful soma- and axon-targeting GABAergic input (Kawaguchi and Kubota, 1993; Miles et al., 1996; Zaitsev et al., 2005).

Grant sponsor: National Institutes of Health (NIH); Grant numbers: EY-08300, EY-015549, EY-017945 (to M.H.); core grant EY P031-13079; NIH NS30989, NS045217, NSF IBN-0314645 (to B.R.).

The first two authors contributed equally to this work.

*Correspondence to: Anita Disney, Center for Neural Science, NYU, 4 Washington Pl., Rm. 809, New York, NY, 10003. E-mail: anita@nyu.edu

Received 4 August 2008; Revised 2 March 2009; Accepted 24 May 2009
DOI 10.1002/cne.22111
Published online June 11, 2009 in Wiley InterScience (www.interscience.wiley.com).

It has been shown that the ability of FS neurons to generate high spike firing frequencies is, at least in part, due to the expression of potassium channels that contain subunits from the Kv3 gene family. Channels that contain Kv3 subunits exhibit distinct electrophysiological properties including relatively high voltages of activation and fast kinetics including rapid deactivation after repolarization (Rudy et al., 1999; Rudy and McBain, 2001). These properties confer neurons with the ability to produce action potentials with narrow spike widths and high firing frequencies in response to constant current steps. These features—narrow spike width and high firing frequencies—in addition to a lack of adaptation to constant current injections, together distinguish FS neurons from interneurons that produce different spiking patterns (i.e., belong to other physiological cell classes). The use of antibodies directed against the Kv3.1b and Kv3.2 subunit proteins has shown that these channel subunits are mainly associated with interneurons in rodent neocortex (Weiser et al., 1995; Chow et al., 1999) but their expression has been studied very little in other mammalian species.

The rodent neocortex may not be a universally applicable neocortical model system—it is known, for example, that PV-ir neurons comprise ≈74% of GABAergic neurons in the primary visual cortex (V1) of macaques (Van Brederode et al., 1990), as opposed to 50% in the rodent neocortex (Gonchar and Burkhalter, 1997). These observations imply that, if PV is a suitable cross-species marker for the FS phenotype, then there is a larger population of FS neurons in area V1 of the macaque than in the neocortex of rodents. Current models of visual processing are relatively well developed (compared with other sensory modalities) and visual tasks are used in experiments designed to examine higher cognitive functions such as those subserving reward and motivation, attention, and memory. Existing visual cortical models have been developed based primarily on experiments conducted on cats and primates. However, the power of genetic techniques has lead to an increase in the use of rodent models for studying the neocortex. Species differences in visual cortical anatomy need to be understood in this context as they may need to be accounted for in modeling the anatomy and physiology of visual systems across species.

Area V1 in macaques is anatomically unique in its inhibitory neuronal population's composition, density, and distribution. For example, throughout the rest of the macaque neocortex, GABAergic interneurons comprise ≈25% of the neuronal population, compared to only 20% in V1 (Beaulieu, 1992). Further, as mentioned above, in V1 74% of GABAergic interneurons express PV (Van Brederode, 1990). This contrasts with PV expression in macaque prefrontal cortex and in the rodent neocortex, where only 50% of GABAergic neurons express PV (Condé et al., 1994; Gonchar and Burkhalter, 1997). While PV is clearly demonstrated to be a marker for FS cells in rodent neocortex, whether PV is a sufficient marker for FS cells in macaque neocortex is uncertain. For example, an immunocytochemical study of Kv3.1b and PV expression in the motor and parietal cortex of macaque monkeys showed that the Kv3.1b subunit is occasionally expressed by pyramidal cells, and also putative inhibitory interneurons that do not express PV (Hartig et al., 1999). Additionally, perineuronal nets, which are anionic extracellular matrices that are believed to support high levels of neuronal firing and that usually ensheath PV-ir FS interneurons in the rodent (Morris and Henderson, 2000), have been found to occasionally ensheath neurons that are PV-immunonegative in the basal forebrain of macaques and humans (Adams et al., 2001), and in the motor and parietal cortices of macaques (Hartig et al., 1999). Finally, in macaque V1 the Kv3.1b subunit is expressed by Meynert cells (Ichinohe et al., 2004), a subset of large glutamatergic pyramidal cells in the deep neocortical layers (Carder and Hendry, 1994).

This study characterizes the laminar and cell type distributions of neurons containing the Kv3.1b and Kv3.2 channel subunits, and relates these distributions to those of the GABAergic population and subpopulations of GABAergic interneurons distinguished by their expression of PV and CB. The results show that the Kv3 subunits are expressed in a much larger population of neurons in macaque V1 than in the rodent neocortex. Notably, we found that ≈25% of both Kv3.1b- and Kv3.2-ir neurons are non-GABAergic, constituting a neuronal class that has not been reported in rodents. Kv3.1b- and PV-ir neurons in V1 also comprise partially nonoverlapping populations in macaque and, finally, Kv3.1b subunits are expressed in CB-ir neurons—results that also contrast with findings in rodents. These data suggest that a broader range of neuronal types may be capable of sustaining high-frequency firing in V1 than would be predicted from data obtained in other model systems.

MATERIALS AND METHODS

Immunocytochemistry

Histological preparation. Seven macaque monkeys (*Macaca fascicularis*) that had been previously used for anesthetized electrophysiological recordings were used in this experiment. Details for the standard protocols of the physiology laboratories can be found in Solomon et al. (2004) and Joshi and Hawken (2006). All procedures were performed in accordance with NIH and institutional guidelines for the care and use of animals. Animals were euthanized with an intravenous (i.v.) injection of sodium pentobarbital (60 mg/kg), and brain death determined by electroencephalogram (EEG). Subsequently, animals were transcardially perfused with heparinized 0.01 M phosphate-buffered saline (PBS, pH 7.4) followed by 4 L of chilled 4% paraformaldehyde (PFA) in 0.1 M phosphate buffer (PB, pH 7.4). Fixative was run for at least 40 minutes. Blocks were removed for track reconstruction for the electrophysiology experiments and the remaining tissue behind a coronal cut at the level of the lunate sulcus was excised and postfixed for 72 hours at 4°C in 4% PFA. The fixed tissue was vibratome-sectioned at 50 μm in the sagittal plane. Every other section was processed for cytochrome oxidase (CO) histochemistry (Wong-Riley, 1979) to create a reference set for determining laminar boundaries (Rockland and Lund, 1983). Remaining sections were stored in PBS with 0.05% sodium azide (PBS-azide) at 4°C.

GABA immunocytochemistry required different fixation procedures. Two additional monkeys (1 *Macaca fascicularis,* 1 *Macaca mulatta*) were used in these experiments. The *fascicularis* was euthanized as described above. The *mulatta* was previously used for chronic electrophysiological recording; the standard protocols for those experiments can be found in Platt and Glimcher (1997). Prior to perfusion the *mulatta* was deeply anesthetized (determined by the abolition

of pedal and corneal reflexes) with an i.v. injection of sodium pentobarbital (60 mg/kg). The animals were both transcardially exsanguinated (as described above) and then a fixative of 1% acrolein / 2% PFA in PB was used. For the *mulatta* (≈13 kg) 75 mL of the acrolein/PFA was used, and for the *fascicularis* (≈5 kg) we used 25 mL (Schwartz et al., 1988; Chow et al., 1999). The animals were then perfused with 2 L of 2% PFA in PB. Chow et al. (1999) specifically investigated fixation procedures to optimize double-labeling for Kv3 and GABA. Schwartz et al. (1988) compared fixation procedures in monkeys (including 4% PFA and 4% PFA plus 1% glutaraldehyde) and found that acrolein allowed for excellent detection of GABA. These previous findings, combined with our own checks of GABA detection (see Antibody Controls, below), indicate that the protocol that we adopted is appropriate for GABA detection. After perfusion, V1 was removed, blocked, and postfixed in 2% PFA for 2 hours and then vibratome-sectioned at 50 μm in the sagittal plane. Sections were then incubated in 1% sodium borohydride in PB for 30 minutes and thoroughly rinsed in PBS. Finally, sections were cryoprotected through a series of washes in dimethyl sulfoxide (DMSO) in PBS (5, 10, 20, 20%) for 10 minutes each and then subjected to 6–8 cycles of a freeze–thaw procedure to improve antibody penetration (Wouterlood and Jorritsma-Byham, 1993). Sections were stored in PBS-azide added at 4°C until processing.

Source and characteristics of primary antibodies. Polyclonal antibodies directed against the Kv3.1 and Kv3.2 potassium channel subunits (anti-Kv3.1b and anti-Kv3.2) were raised in rabbits according to protocols described by Chow et al. (1999) and Weiser et al. (1994). The anti-Kv3.1 was specific to the Kv3.1b subunit (Weiser et al., 1995; Sekirnjak et al., 1997)—amino acids 567–585 of the mouse Kv3.1b channel subunit were used as an immunogen. The anti-Kv3.2 was raised against amino acids 171–189 of the mouse Kv3.2 channel subunit. These antigenic sites are homologous with sites on the macaque Kv3.1b (predicted 100% homologous with mouse) and Kv3.2 (100% homologous with mouse) channel subunits.

The monoclonal anti-GABA antibody was raised in mouse against GABA conjugated to bovine serum albumin (BSA; Cat. no. A0310, lots 042K4817 and 123K4793: Sigma, St. Louis, MO). The polyclonal goat anti-parvalbumin antibody (gt-anti-PV: Cat. no PVG-214, lot 3.6; Swant, Bellinzona, Switzerland) and the polyclonal rabbit anti-parvalbumin antibody (rb-anti-PV: Cat no PV-28, lot 5.5; Swant) were both raised against rat muscle parvalbumin. The monoclonal mouse anti-calbindin-D28K antibody (ms-anti-CB: Cat. no. 300, lot 18F; Swant) and the polyclonal rabbit anti-calbindin D-28K (rb-anti-CB: Cat no. CB-38, lot 5.5; Swant) were both raised against recombinant rat calbindin.

The selectivity of the anti-Kv3.1b and anti-Kv3.2 antibodies has been demonstrated in rodents by immunoblots (Weiser et al., 1995; Chow et al., 1999) and immunoprecipitation (Chow et al., 1999). The antibodies have been shown to label single bands at ≈80–90 kD (anti-Kv3.1b) and ≈100 kD (anti-Kv3.2). Selectivity was further confirmed by an absence of immunoreactivity in immunoblots on tissue homogenates from Kv3.1b and Kv3.2 knockout mice (Ho et al., 1997; Lau et al., 2000), and immunocytochemistry in tissue sections from Kv3.2 knockout mice (Lau et al., 2000). Preadsorption and Western blot control experiments were performed on tissue from macaque V1 (these data are described in Antibody Controls, below).

The anti-GABA was characterized by dot blot immunoassays. No crossreactivity was observed with L-α-aminobutyric acid, L-glutamic acid, L-aspartic acid, glycine, δ-aminovaleric acid, L-threonine, L-glutamine, taurine, putrescine, L-alanine, and carnosine (Sigma product information, Cat. no. A-0310). The immunogen used to make the anti-GABA was a GABA-BSA complex. We used BSA in our antibody dilutent, and this did not adsorb out the GABA staining.

The rb- and ms-anti-CB antibodies have been characterized by immunoblot and radioimmunoassay on tissue homogenates and shown to label a single protein band of 28 kDa (Celio et al., 1993). Importantly, these antibodies do not cross-react with calretinin (Celio et al., 1993). The gt- and rb-anti-PV have been characterized by Western blot on rodent brain homogenate and labels a single band at ≈12 kDa (E. Celio, pers. commun.). In tissue sections from macaque V1, preadsorption against saturating concentrations of the target antigen (full-length PV or CB, purchased from Swant) abolished immunolabeling for both the CB and PV antibodies (Disney and Aoki, 2008).

Immunoperoxidase labeling. Sections were processed to detect immunoreactivity for Kv3.1b or Kv3.2 channel subunits using the ABC-DAB method (Hsu et al., 1981). Between 3 and 10 sections per animal were selected pseudorandomly for immunocytochemical processing for each experiment. First, the tissue was incubated in 1% hydrogen peroxide in PBS for 30 minutes. After PBS rinses, the tissue was incubated for an hour in blocking solution A; consisting of 0.2% Triton X-100 (Triton), 10% normal goat serum (Jackson ImmunoResearch, West Grove, PA), 0.2% coldwater fishskin gelatin (Sigma), and 1% BSA (Jackson ImmunoResearch) in PBS. Next the tissue was incubated overnight in primary polyclonal antibodies directed against either the Kv3.1b (1:1,000 in BS) or Kv3.2 (1:200 in BS) channel subunits, diluted in blocking solution A.

Following primary antibody incubation sections were rinsed in PBS and incubated in a biotinylated goat antirabbit IgG antibody (1:100 in blocking solution: Vector Laboratories, Burlingame, CA) for 1 hour. The sections were then rinsed in PBS and transferred into an avidin-horseradish peroxidase (HRP) complex solution (Vectastain Elite ABC Kit, Vector Laboratories) for 30 minutes. After rinsing in PBS, sections were incubated in 50 mL of PBS, 11 mg 3,3′-diaminobenzidine HCl (DAB; Aldrich Chemical, Milwaukee, WI) with 5 μL hydrogen peroxide (30%) until cell bodies were distinguishable when viewed under a low-power microscope. The sections were rinsed in PBS, mounted, and dried overnight before dehydration and coverslipping (Permount: Fisher Chemicals, Pittsburgh, PA).

Reference sections processed to visualize CO were incubated at 4°C in a solution of 4% sucrose in PB on a shaker. They were then transferred into PB with 4% (w/v) sucrose, 0.02% catalase (Sigma), 0.03% cytochrome C (Sigma), and 0.05% DAB (Aldrich) and placed in an oven on a shaker. The tissue was maintained at 37–39°C for up to 48 hours. The solution was refreshed after the first 24 hours if needed. The tissue was removed when the highly reactive and nonreactive cytochrome oxidase patches in layers 2 and 3 were clearly differentiated. The sections were rinsed in PBS, mounted, dried, dehydrated, and coverslipped using Permount (Fisher).

Immunofluorescence: dual-labeling. Dual labeling to visualize the Kv3s with PV and with CB was achieved by first incubating sections in blocking solution B consisting of 0.4% Triton, 1% BSA (Jackson ImmunoResearch), 5% normal chicken serum (Jackson ImmunoResearch), 0.4% Coldwater fishskin gelatin (Sigma), and 0.05% sodium-azide in PBS for 1 hour. Sections were then incubated overnight at room temperature in gt-anti-PV or ms-anti-CB diluted at 1:1,000 in blocking solution B. The next day sections were thoroughly rinsed in PBS and incubated in a chicken antigoat IgG or chicken antimouse IgG secondary antibody conjugated to the Alexa 488 fluorophore (Invitrogen, La Jolla, CA; A21467 lot 93C3, and A21200 lot 73C2, respectively) used at 10 μg/mL in 1% BSA in PBS for 4–6 hours in the dark on a shaker. From this point on, tissue transfers were done in low light conditions and incubations proceeded in darkness, to protect the fluorescent signal. The PV or CB single-labeled sections were rinsed in PBS and incubated in either rabbit anti-Kv3.1b (1:1,000) or rabbit anti-Kv3.2 (1:100) in 0.05% BSA in PBS overnight. The sections were rinsed again and incubated in a chicken antirabbit IgG conjugated to the Alexa 594 fluorophore (Invitrogen, A21442 lots 49950 and 42797) used at 10 μg/mL in 1% BSA in PBS for 4–6 hours on a shaker. The sections were rinsed and mounted, dried, and coverslipped with DPX mounting medium (Electron Microscopy Services, Fort Washington, PA).

Processing to visualize Kv3/GABA-ir proceeded as above, except Triton was omitted from the blocking solution to prevent GABA washout. The freeze–thaw process described above (see Histological Preparation) was used in the place of Triton to permeabilize the tissue for GABA detection. The anti-GABA antibody was used at 1:100.

Antibody controls.

Primary antibodies.

Preadsorption controls were performed for the anti-Kv3.1b and anti-Kv3.2 antibodies. Recombinant Kv3.1b [CKESPVIAKYMPTEAVRVT] and Kv3.2 [CTPDLIGGDPGDDEDLAAKR] peptides produced in *E. coli* (purified peptides purchased from GenScript (Piscataway, NJ), lots 427800112255 and 405200010913, respectively) were diluted at 100 μM in the premixed antibody solution. Effectiveness of preadsorption was assessed by ABC-DAB (Hsu et al., 1981). Preadsorption completely eliminated staining for Kv3.1b and Kv3.2, although we observed Kv3.1b- and Kv3.2-ir in tissue sections that were simultaneously processed according to the normal protocols (Fig. 1a–d).

Western blots were also performed on V1 tissue homogenates from two macaques (Fig. 1e). The antibodies detected single, diffuse bands at ≈80–90 kD (Kv3.1b) and ≈100 kD (Kv3.2). These molecular weights are similar to those seen in rat and mouse brain (Weiser et al., 1995; Chow et al., 1999). The breadth of the bands in all three species is likely to reflect the existence of multiple splice variants (Kv3.2) and heterogeneity of posttranslational modifications (Kv3.1b and Kv3.2).

Secondary antibodies. For each set of experiments we performed controls to confirm the specificity of the secondary antibodies by incubating tissue sections in solutions without primary antibodies (no primary control). In these controls, tissue sections were incubated overnight in blocking solution only and subsequently processed according to the regular protocols. This incubation produced no fluorescent signal.

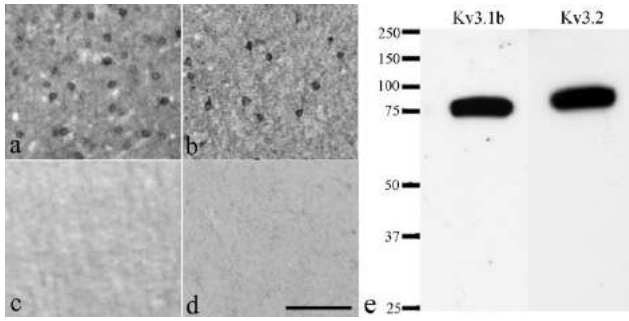

Figure 1.
Kv3 antibody controls on V1 tissue. **a,b:** Macaque V1 tissue processed to detect Kv3.1b (a) or Kv3.2 (b) immunoreactivity by an ABC-DAB reaction. Preadsorption of the antibodies against a saturating concentration of the target antigen (see Antibody Controls) abolished staining for both the Kv3.1b **(c)** and Kv3.2 **(d)** subunit proteins. **e:** Immunoblots on macaque V1 tissue homogenates treated with Kv3.1b (left lane) and Kv3.2 (right lane) antibodies show that each antibody labels a single broad protein band. Scale bar = 100 μm.

We also conducted a control experiment in which we incubated tissue sections, which had been tagged with a primary antibody, in solution containing a secondary antibody that targeted a different species than the host animal in which the primary antibody was raised (mismatched secondary control). In other words, the secondary antibody had no target epitope in the tissue, and we confirmed that this incubation produced no fluorescent signal.

Control studies for antigen detection.

Kv3-ir neurons.

To ensure that the detection of Kv3-ir neurons was consistent across experimental conditions a comparison was made of the detection rates for Kv3-ir neurons in tissue processed for immunofluorescence and immunoperoxidase labeling. Using the confocal microscope, photomicrographs were taken of the opercular surface of fluorescently labeled tissue from two animals in columns extending from the pial surface to the white matter (100×). A grid (140 × 140 μm) was superimposed onto the photomicrographs and a nonstereological count of the number of neurons that occurred within that area was performed. This process was repeated, using photomicrographs taken using a compound microscope, for immunoperoxidase-labeled tissue. The detection rate of Kv3-ir neurons was found to be comparable between the processing conditions.

GABA-ir neurons. To examine whether the immunofluorescence protocol resulted in adequate detection of GABA-ir neurons, confocal images were taken of 50 μm-wide columns extending from the pial surface into the white matter, and a comparison of a nonstereological count of the number of cells per column was made with a similar count reported by Hendry et al. (1987). In tissue from two animals, three columns were imaged from two sections per animal (six columns/animal). The average numbers of cells per column for each animal (57.33, 65.5) were within the range (52–66) that Hendry et al. (1987) reported.

Additionally, immunofluorescent dual-labeling studies were performed to compare the detection of GABA-ir neurons to the detection of PV- and CB-ir neurons (the latter as a "cocktail" incubation with a single label). Tissue was processed as described above for PV/Kv3 and CB/Kv3 dual labeling, except

that in the first step the tissue was incubated in a single solution with both rb-anti-PV and rb-anti-CB. Therefore, PV- and CB-ir neurons were tagged with the same fluorescent marker (i.e., a single secondary antibody was used to label both primary antibodies, which were raised in the same host species) and GABA-ir neurons were tagged with a different fluorescent marker. Three photomontages were taken from two animals on the confocal microscope (63×). Out of 137 peptide-ir neurons, 134 were also GABA-ir, showing that our protocols detect at least 97.8% of GABAergic neurons. This actually represents a lower bound on the detection of GABAergic neurons because a small population of CB-ir neurons is probably non-GABAergic (Van Brederode et al., 1990; Disney and Aoki, 2008).

Analysis

Stereological quantification of Kv3.1,2-ir cells. The laminar numerical densities (N_v) of cells expressing Kv3.1b and Kv3.2 subunits were determined using the optical disector method (Sterio, 1984; Mouton, 2002). First, tissue shrinkage in the z-axis (Majlof and Forsgren, 1993) was estimated using a calibrated microscope stage. The nominal tissue thickness (50 μm) was divided by the number of incremental steps that could be taken through the section. We were then able to relate an incremental step of the microscope stage to a discrete progression in the z-axis of the tissue. In this way, movements through the depth of the tissue could be performed in a manner that compensated for shrinkage, enabling more accurate estimates of the size of each optical disector (Skoglund et al., 1996). We only counted somata, not proximal dendrites. Cells were counted from photomicrographs (see Photomicrograph Production, below) using Photoshop CS (Adobe Systems, San Jose, CA). Only clearly labeled somata were counted, without regard to the labeling or visibility of proximal dendrites. Cells were only counted if at least two-thirds of a continuous cytoplasmic or membranous ring was visibly immunoreactive around the nucleus. Punctate labeling around a soma in the absence of visible cytoplasmic immunoreactivity was not included because the resolution of the microscopes used in this study does not allow us to disambiguate pre- versus postsynaptic immunoreactivity. As such, these stereological counts should be viewed as a lower bound on the true size of the population of Kv3-ir neurons.

Counts were made from montages of light micrographs—extending in columns from the pial surface to the white matter—of the opercular surface of V1 using a 40× objective. Each region of tissue in the column was imaged in two focal planes: the micrographs of these two planes for an area of tissue (50 × 50 μm or 50 × 40 μm) constituted a single disector. For each Kv3 channel, at least 1,200 disectors were analyzed from each of three animals. The distance from the deepest boundary of each dissector to the pial surface was noted. Adjacent CO reference sections were used to determine the laminar location of the disectors.

Superimposing images of adjacent sections showed that shrinkage in the x- and y-axes of tissue processed to visualize the Kv3 channels was comparable to shrinkage in the CO sections. Therefore, no accommodation for x-y shrinkage was made when using laminar depth measurements from the CO sections.

To test whether the anti-Kv3.1b and anti-Kv3.2 antibodies penetrated the full depth of the tissue, we performed random cell counts using a 40× objective in three animals per antibody. Counts were made at a minimum of 10 depths through each tissue section (depending on shrinkage, increments corresponded to steps of 4–5 μm). The number of cells encountered remained constant at each depth (40 ± 7 cells). Specifically, there were no systematic differences in the cell counts at depths that corresponded to the middle of the section (as would be expected from incomplete antibody penetration). Therefore, we concluded that the anti-Kv3 antibodies fully penetrated the tissue sections.

The dual-labeling study was not stereological and so the Abercrombie correction (T/T+h: see Guillery, 2002) was applied to reduce the counting bias associated with soma size. For Kv3.1b-ir and Kv3.2-ir neurons, object height (h) was measured as the average diameter along the long axis of the nonimmunoreactive region visible within the cell soma. This average was calculated based on measuring 24 Kv3.1b-ir neurons (including two layer 4b bipolars and one Meynert cell), resulting in a mean h of 7.53 μm. Twenty-one Kv3.2-ir neurons were measured, resulting in a mean h of 6.23 μm. For GABA-, PV-, and CB-ir neurons, h was measured from the DAPI-stained nuclei of 48 GABA-ir, 37 PV-ir, and 13 CB-ir neurons from on sections mounted using Vectashield with DAPI mounting medium (Vector). This resulted in a mean h of 7.17 μm for GABA, 7.32 μm for PV, and 6.97 μm for CB. For counts involving anti-GABA, section thickness (T) was adjusted to 19.2 μm (the mean depth of penetration calculated from 10 tissue sections) to reflect the incomplete penetration of the tissue by the antibody (and thus the region of tissue analyzed). For the other antibodies, the entire tissue thickness was penetrated by the antibodies and so the mean dehydrated thickness of the tissue was used (measured as the distance between the upper- and lower-most in-focus planes), giving a T of 42.49 μm. The resulting Abercrombie correction factors were 0.728 (GABA-ir neurons), 0.853 (PV), 0.859 (CB), 0.718 (Kv3.1b when counted with GABA), 0.849 (Kv3.1b when counted with PV or CB), 0.755 (Kv3.2 when counted with GABA), and 0.872 (Kv3.2 when counted with PV or CB). Both raw and corrected counts are reported in the text; percentages are calculated based on the corrected numbers.

Epifluorescence/confocal microscopy and cell counting. For reasons described in detail below, to achieve accurate cell counts it was necessary to vary the counting method between data sets. Briefly, when PV- and CB-ir neurons were the base populations that were counted (i.e., in determining the percentage of PV and CB neurons that were single- and dual-labeled) an epifluorescence microscope was used, with a 100× oil immersion lens, and cells were examined through all the depths of the tissue by manually moving through the z-axis in both fluorescent channels. When GABA-ir neurons were the base population, the same method was adopted but only at the surface of the tissue section, in the region fully penetrated by the GABA antibody. When Kv3.1b- and Kv3.2-ir neurons were the base populations, neurons were counted from photomicrographs taken on the confocal microscope. Montages of photomicrographs were taken of the opercular surface of V1 in columns extending from the pial surface to the white matter using either a 63× or 100× oil-immersion objective. Images were later analyzed using Photoshop CS (Adobe).

Importantly, for each cell type, percentages of single- and dual-labeled cells were calculated from data collected using a

TABLE 1. Summary of Counting Methods

Value	Numerator	Denominator	Method	Reason for not using full confocal
% Kv3 (single or dual labeled with PV)	# Kv3-ir neurons (single OR dual labeled)	# Kv3 single labeled neurons AND Kv3/PV dual labeled neurons	Full confocal	
% Kv3 (single or dual labeled with CB)	# Kv3-ir neurons (single OR dual labeled)	# Kv3 single labeled neurons AND Kv3/CB dual labeled neurons	Epifluorescence	* Field of view of confocal too small to efficiently sample the sparse CB-ir population
% Kv3 (single or dual labeled with GABA)	# Kv3-ir neurons (single OR dual labeled)	# Kv3 single labeled neurons AND Kv3/GABA dual labeled neurons	Confocal at surface of tissue sections	* Limited penetration of GABA antibody
% PV (single or dual labeled with Kv3	# PV-ir neurons (single OR dual labeled)	# PV single labeled neurons AND PV/Kv3 dual labeled neurons	Epifluorescence	* Restricted Kv3 signal in z axis
% CB (single or dual labeled with Kv3)	# CB-ir neurons (single OR dual labeled)	# CB single labeled neurons AND CB/Kv3 dual labeled neurons	Epifluorescence	* Restricted Kv3 signal in z axis
% GABA (single or dual labeled with Kv3)	# GABA neurons (single OR dual labeled)	# GABA single labeled neurons AND GABA/Kv3 dual labeled neurons	Epifluorescence at surface of tissue sections	* Limited penetration of GABA antibody * Restricted Kv3 signal in z axis

Although counting somata from confocal micrographs was the preferred method of data collection in this study, some of the staining patterns produced by the different antibodies would have created a systematic bias in counts collected in this way. Therefore, the counting method was adjusted by dataset to correct for biases produced by antibody staining patterns. This table summarizes the counting methods and calculations that were used to determine the population percentages from each dataset, and the reasons for choosing each method. For all of the counts the percentages reported for each cell type was calculated from data collected by a single method. For example, for Kv3.1b/PV dual-labeled tissue the percentage of Kv3.1b single-labeled neurons was calculated as the number of Kv3.1b single-labeled neurons counted from confocal micrographs divided by the number of all Kv3.1b-ir neurons, both single- AND dual-labeled with PV, counted from confocal micrographs.

single method. For example, for Kv3.1b/GABA dual-labeled tissue, the percentage of Kv3.1b single-labeled neurons was calculated as the number of Kv3.1b single-labeled neurons counted from confocal micrographs divided by the number of all Kv3.1b-ir neurons, both single- and dual-labeled, counted from confocal micrographs. The percentage of GABA single-labeled neurons, conversely, was calculated as the number of GABA single-labeled neurons counted under epifluorescence divided by the number of all GABA-ir neurons, both single- and dual-labeled, counted under epifluorescence (see Table 1). Further details of the methods that were adopted and the reasons behind these choices follow.

The immunofluorescent signal filled the volume of the soma for almost all PV-, CB-, and GABA-ir neurons, but Kv3-ir was often restricted to a small region of the soma. Under such circumstances, dual-labeling could easily be missed as a result of the thin optical sectioning offered by the confocal microscope (Fig. 2). Therefore, to determine the percentage of PV-, CB-, and GABA-ir cells that were dual-labeled with Kv3, each PV-, CB-, or GABA-ir labeled cell was examined in all depths of the tissue for Kv3 label by manually moving through the z-axis using an epifluorescence microscope.

The method for counting Kv3-ir neurons differed by dataset. Tissue processed for Kv3/GABA-ir showed unequal tissue penetration by the two primary antibodies. While the anti-Kv3.1b and anti-Kv3.2 penetrated the tissue throughout its depth, the anti-GABA did not fully penetrate the tissue sections. For these datasets, neurons were counted from photomicrographs taken using the confocal microscope. The focal plane of each image was chosen using the channel showing GABA-ir. To count Kv3-ir neurons in Kv3/PV dual-labeled tissue neurons were counted from confocal photomicrographs from any depth of the tissue (as both antibodies penetrated the tissue fully). In Kv3/CB dual-labeled tissue the CB-ir population was relatively sparse and the field of view of the confocal microscope was too small to efficiently sample this population. Therefore, for the Kv3/CB dataset, Kv3-ir neurons were counted using epifluorescence (Table 1).

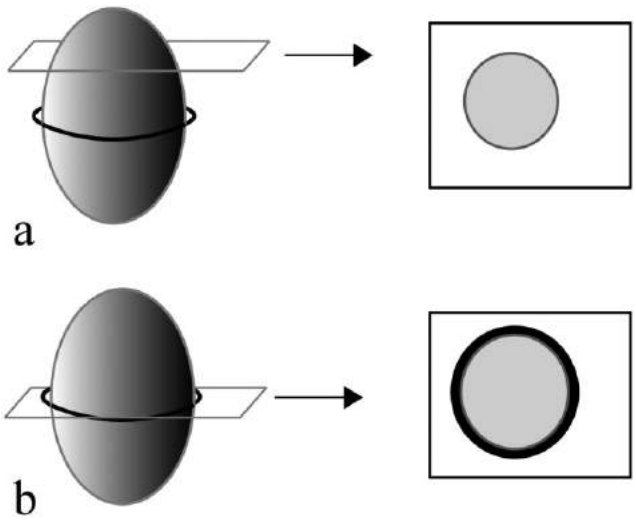

Figure 2.
The use of epifluorescence to count certain cell populations. Kv3 immunoreactivity often appeared as a ring in a restricted plane of the tissue, illustrated here as a black ring around a grayscale neuron. While Kv3 labeling was not only observable at the equator of cells, for many cells labeling was less readily observable at other regions of the cell surface. Therefore, for counts of cells that were dual-labeled for Kv3 subunits and another protein, it was necessary to scan through the full soma of labeled neurons. Had the counts of GABA-, CB-, or PV-ir neurons, for which the immunofluorescent signal filled the volume of immunopositive somata, been conducted using single-plane images, these images would have frequently shown cells in a plane that incorrectly appeared to be Kv3-immunonegative. This counting method would have resulted in an overestimation of the number of neurons that were single-labeled for GABA-, CB-, or PV-immunoreactivity **(a)**. Using single-plane images (i.e., confocal micrographs), we would have only correctly identified a cell as dual-labeled if the image were taken in the precise plane in which the Kv3 signal appeared **(b)**. For this reason, when counting the GABA-, PV-, or CB-ir populations it was necessary to examine both fluorescent channels, the tissue throughout the depth of the section. This was done using an epifluorescence microscope.

When Chow et al. (1999) performed a comparable analysis of the coexpression of Kv3.1b and K3.2 with GABA and the calcium-binding proteins in the rodent neocortex, they pooled data from layers 2–4 and from layers 5 and 6. Although these laminar divisions are not ideal for an analysis of macaque V1, applying these divisions was practicable and allowed our data to be directly compared to the data collected from the rodent brain. The border between layers 4c and 5 was determined by qualitative criteria. Specifically, layer 4c appears more opaque in fluorescence due to dense white matter projections, and is more densely populated than layer 5, so the layer transition was easily identified. Additionally, the cell populations labeled for PV, CB, and GABA are expressed differently between the layers (Van Brederode et al., 1990; Beaulieu et al., 1992; Disney and Aoki, 2008). GABA- and PV-ir neurons are very numerous in layer 4c, and occur much more sparsely in layer 5. CB, conversely, is rarely expressed in neurons in layer 4c and is frequently expressed in neurons in layer 5. In cases in which we were able to coregister a fluorescent section with its adjacent CO section, we compared the boundary that we qualitatively determined with the layer 4c/5 boundary in the CO section. By this method we were able to confirm that we could accurately identify this boundary using our qualitative criteria.

Qualitative data collection. Qualitative data were collected from the same photomicrographs that were used to collect quantitative data. For nonsomatic staining the term "neuropil staining" will be used. Neuropil staining includes axonal, dendritic, and punctate labeling. Axons were identified according to the presence of clearly distinguishable varicosities resembling "beads on a string." Dendrites were identified as processes of a slightly varicose or nonvaricose nature. Additionally, we identified puncta as small spots, $\approx$1 μm or less, that were not clearly attached to a neuronal process. These puncta could represent spines, axon terminals, or "islands" of immunoreactivity along larger processes such as dendrites or axons.

Photomicrograph production. Digital light micrographs were captured using an Olympus Microfire Camera and Optronics Imaging Software. Brightness and contrast settings were chosen independently for each image prior to data collection using a live color image. The brightness and contrast were deemed optimal when artifacts from the vasculature appeared white and the reddish-brown DAB-reaction product appeared as the same intensity that was observable under the compound microscope. Micrographs were analyzed using Photoshop CS (Adobe). Published images were adjusted to equalize contrast and brightness; no other alterations were made.

Digital confocal micrographs were captured using a Zeiss LSM 310 confocal microscope. Brightness and contrast settings were chosen independently for each image using a live false color (red) image. The brightness and contrast settings were deemed optimal when artifacts from the vasculature appeared black and the strongest labeling in the field of view appeared yellow. No adjustment of the brightness of the pixels was made in between these points (gamma adjustment). All micrographs were analyzed using Photoshop CS (Adobe). Cell counting was done on isolated red/green images before conversion to magenta/green images for publication.

Dual in situ hybridization/immunocytochemistry

RNA probe design and labeling. Antisense RNA probes were prepared for the 67 kDa glutamic acid decarboxylase (GAD67) and for the α subunit of calcium/calmodulin dependent protein kinase II (CaMKIIα). The cloning of cDNAs encoding subunit fragments was obtained by polymerase chain reaction (PCR) from macaque cortex cDNA using [CamK: GAAGCTGTCAGCCAGAGACC, ACTGAACGCTGGAACTGGAC Gad67: GCTGTGCCCAAACTGGTACT, TTACAGATCCTGGCCCAGTC]. The thermocycler protocol for PCRs was as follows: 94°C, 1 minute; 60°C, 1 minute; 72°C, 1 minute; for 30 cycles. Single-stranded cDNA was prepared from random-primed total RNA using SuperScript III Reverse Transcriptase (Invitrogen) as described previously (Saganich et al., 1999).

Each PCR amplification product was cloned into PCDNA4 (Invitrogen), linearized with NotI and a template for in vitro transcription prepared by Purification using QIAquick PCR cleanup (Qiagen, Chatsworth, CA) under RNAase free conditions. Antisense digoxigenin (DIG)-labeled RNA probes (Roche, Hertforshire, UK) were made following the manufacturer's protocol by in vitro transcription in the presence of DIG-labeled UTP (Roche) using $\approx$3 μg of template and T3 RNA polymerase (Roche).

The integrity of each RNA probe was analyzed by gel electrophoresis (Embi Tec, San Diego, CA), and the level of DIG-UTP incorporation was tested by dot blot by comparison to a known DIG-labeled RNA standard (Roche). For each probe the transcription reaction resulted in 20 μL of DIG-labeled RNA, which was diluted with RNAase-free H_2O (Sigma) to 400 μL, aliquoted, and stored at −80°C.

To avoid possible crossreactivity, each probe was designed to include regions of low nucleotide identity with other sequences located in the National Center for Biotechnical Information nucleotide database.

Combined in situ hybridization-immunohistochemistry. The nonradioactive (NR)-ISH protocol used has been described previously (Saganich et al., 2001). Briefly, macaques (*Macaca fascicularis*) were transcardially exsanguinated with cold PBS and perfused 4% PFA. Blocks of V1 tissue were removed and postfixed for 1 hour before being placed in 30% sucrose for 48 hours. The tissue was sectioned on a freezing-microtome at 40 μm thickness and floating sections were prehybridized at 60°C in a solution containing 60% formamide (Sigma), 3.5× sodium chloride/sodiumcitrate (SSC; Invitrogen), 5% dextran sulfate (Chemicon, Temecula, CA), 3.5× Denhardt's solution (Roche), 0.5 mg/mL denatured salmon sperm DNA (Sigma), 0.2 mg/mL t-RNA (Roche), and 0.25 mg/mL SDS. After 1 hour of prehybridization, 50 ng/mL of DIG-labeled RNA probe was added and the hybridization reaction was allowed to proceed for 17 hours.

After hybridization the sections were washed in decreasing concentrations of SSC buffer (2× to 0.1×) at 65°C followed by a single wash in buffer B1 (150 mM NaCl, 100 mM Tris, pH 7.4) at room temperature. Sections were then treated for 1 hour at room temperature in buffer B1 + 10% normal sheep serum (Jackson) followed by overnight incubation at 4°C with anti-DIG Fab fragments conjugated with alkaline phosphatase (AP, Roche) in buffer B1 + 1% normal sheep serum. Antibodies directed against Kv3.1b channel subunits (diluted 1:1,000) were added with the anti-DIG antibodies. Overnight incubation with antibodies was followed by three 15-minute washes in buffer B1 sections at room temperature in buffer B1 followed by a single wash in DIG detection buffer (100 mM NaCl, 100 mM Tris, 50 mM $MgCl_2$, pH 9.5). DIG detection was per-

formed using the AP substrate nitro blue tetrazolium/5-bromo-4-chloro-3-indolyl phosphate (NBT/BCIP; Roche) for 6–8 hours in DIG detection buffer. The reaction was stopped by rinsing sections four times for 15 minutes in ddH_2O. After AP detection was complete, sections were washed three times for 15 minutes in buffer B1, followed by a 2-hour incubation at room temperature with secondary antibodies (anti-rabbit Cy3; Molecular Probes, Eugene, OR) in buffer B1 + 1% normal goat serum + 0.1% BSA + 0.02% cold water fish gelatin. After treatment with secondary antibodies, sections were mounted in 0.1× SSC, partially dried, and coverslipped in Vectashield with DAPI (Vector) on glass slides. Images were acquired using an Olympus Provis microscope equipped with a MagniFire digital camera. Fluorescent images were acquired using filter sets for Cy3.

RESULTS

In rodents, ≈50% of all GABAergic neurons express PV (Gonchar and Burkhalter, 1997) and >99% of these PV-ir neurons express Kv3.1b potassium channel subunits. Studies in rodent neocortex suggest that Kv3.1b subunits form the channels that underlie the FS behavior of these PV-ir neurons (Erisir et al., 1999), although similar studies have not been conducted in primate cortex. In macaque V1, ≈74% of GABAergic neurons express PV. It is not known whether the higher prevalence of PV-ir neurons indicates that there is a larger population of FS neurons in V1 of macaques, or whether some PV-ir neurons in this area are not FS. To begin answering these questions, in this study we used stereological methods to reveal the laminar densities of Kv3.1b- and Kv3.2-ir neuronal somata and compared these densities with that of neurons expressing GABA. We also used dual immunofluorescence techniques to directly examine coexpression of GABA, PV, and CB with the Kv3.1b and Kv3.2 subunits. In doing so, we found evidence that there are non-GABAergic neurons in macaque V1 that express Kv3.1b and Kv3.2 subunits, a result that contrasts with observations made of the rodent neocortex. Also at odds with data from rodents, we found a population of PV-ir neurons that do not express Kv3.1b subunits (however, these cells may express the Kv3.2 subunit; see Discussion), as well as Kv3.1b-ir neurons that do not express PV. Finally, we found evidence for a population of inhibitory cells expressing CB (but not PV) that are immunoreactive for Kv3.1b and/or Kv3.2 channels subunits.

Kv3.1b immunoreactivity profile

Across all layers of macaque V1, tissue processed to visualize Kv3.1b antigenic sites showed punctate neuropil staining, although the neuropil immunoreactivity was most intense in layers 1–4b (Fig. 3a). Somatic Kv3.1b-ir was also observed in all layers, but appeared more prominent in layers 5 and 6 in the low-power micrograph because of the fainter neuropil staining in these layers (Fig. 3a).

In individual neurons, Kv3.1b-ir was localized to the somatic periphery, close to the plasma membrane (Fig. 4a). In most immunopositive neurons there was weak staining of the very proximal dendrites but very little or discontinuous staining of major dendritic or proximal axonal processes. As a result, it was not possible to make morphological characterizations of most of the Kv3.1b-ir neurons. However, there were some exceptions. Meynert cells, a morphologically distinct class of pyramidal neurons with large somata (circumference ≈72–74 μm; Vogt Weisenhorn et al., 1995) that reside near the border between layers 5 and 6, showed Kv3.1b-ir of their somata and proximal dendrites (Fig. 4b). Additionally, large bipolar and multipolar cells in layers 4b, 5, and 6 showed Kv3.1b-ir of their somata and faint staining of their proximal dendrites (Fig. 4c,d). Kv3.1b was also faintly expressed in vertically oriented dendrites in the upper part of layer 2, running perpendicular to the pial surface (Fig. 5a,b). These are probably the cut dendrites from Kv3.1b-ir somata not in the tissue section. Axonal expression of Kv3.1b was difficult to confirm due to the darkness of neuropil-immunoreactivity, but a few thin, beaded, immunopositive processes were observed, resembling axons with varicosities (Fig. 5c).

Kv3.2-ir profile

Kv3.2-ir in the neuropil occurred in all layers of cortex, although neuropil staining was darker in layers 2 and 3 than in layers 4a–6 (Fig. 3b).

Within individual neurons, Kv3.2 expression was, like Kv3.1b-ir, largely restricted to the somatic periphery. The darkest somatic staining was observed in neurons in layers 5 and 6. Although somatic staining appeared less intense in neurons of layers 2–4 in the low-power micrograph (Fig. 3b) the staining was easily discerned at higher power (Fig. 6a). Due to poor labeling of proximal processes it was not possible to identify morphological types among the Kv3.2-ir neurons. Notably, Meynert cells, whose large somata would allow them to be identified even in the absence of labeled processes and which expressed Kv3.1b, did not express Kv3.2. There was no obvious dendritic Kv3.2 expression; however, occasionally Kv3.2-ir was observed in axons (Fig. 6b).

Quantitative laminar distribution of Kv3.1b- and Kv3.2-ir somata

The density of Kv3.1b-ir somata in each layer (laminar density) was quantified to allow us to compare our results with published data on the laminar density of all neurons, GABAergic interneurons, and subpopulations of GABAergic interneurons identified by their expression of calcium-binding proteins. Such a comparison demonstrates the relative abundance of neurons expressing Kv3.1b and shows that these neurons outnumber GABAergic neurons.

The numbers of neurons that somatically expressed Kv3.1b were quantified by stereological methods. The highest density of Kv3.1b-ir somata occurred in layers 2–4c (Fig. 7, Table 2). A comparison was made between the distribution of Kv3.1b-ir neurons and the laminar distribution of GABA-ir interneurons obtained from a study by Beaulieu et al. (1992) that used comparable stereological methods. In layer 2/3, the density of Kv3.1b-ir neurons (39,000/mm^3) exceeds the density of GABAergic interneurons (28,200/mm^3; Beaulieu et al., 1992). The differences are even more pronounced in layer 4b, in which the density of Kv3.1b-ir neurons (41,400/mm^3) is more than twice the density of GABAergic interneurons (20,400/mm^3; Beaulieu et al., 1992). And finally, in layer 4c, the Kv3.1b-ir population (33,800/mm^3) also outnumbers the population of GABAergic interneurons (27,233/mm^3; Beaulieu et al., 1992). In contrast, the density of Kv3.1b-ir somata in layers 5 and 6 (18,700/mm^3, 14,200/mm^3, respectively) is lower than the density of the GABAergic population (22,300/mm^3, 16,500/mm^3, respectively; Beaulieu et al., 1992).

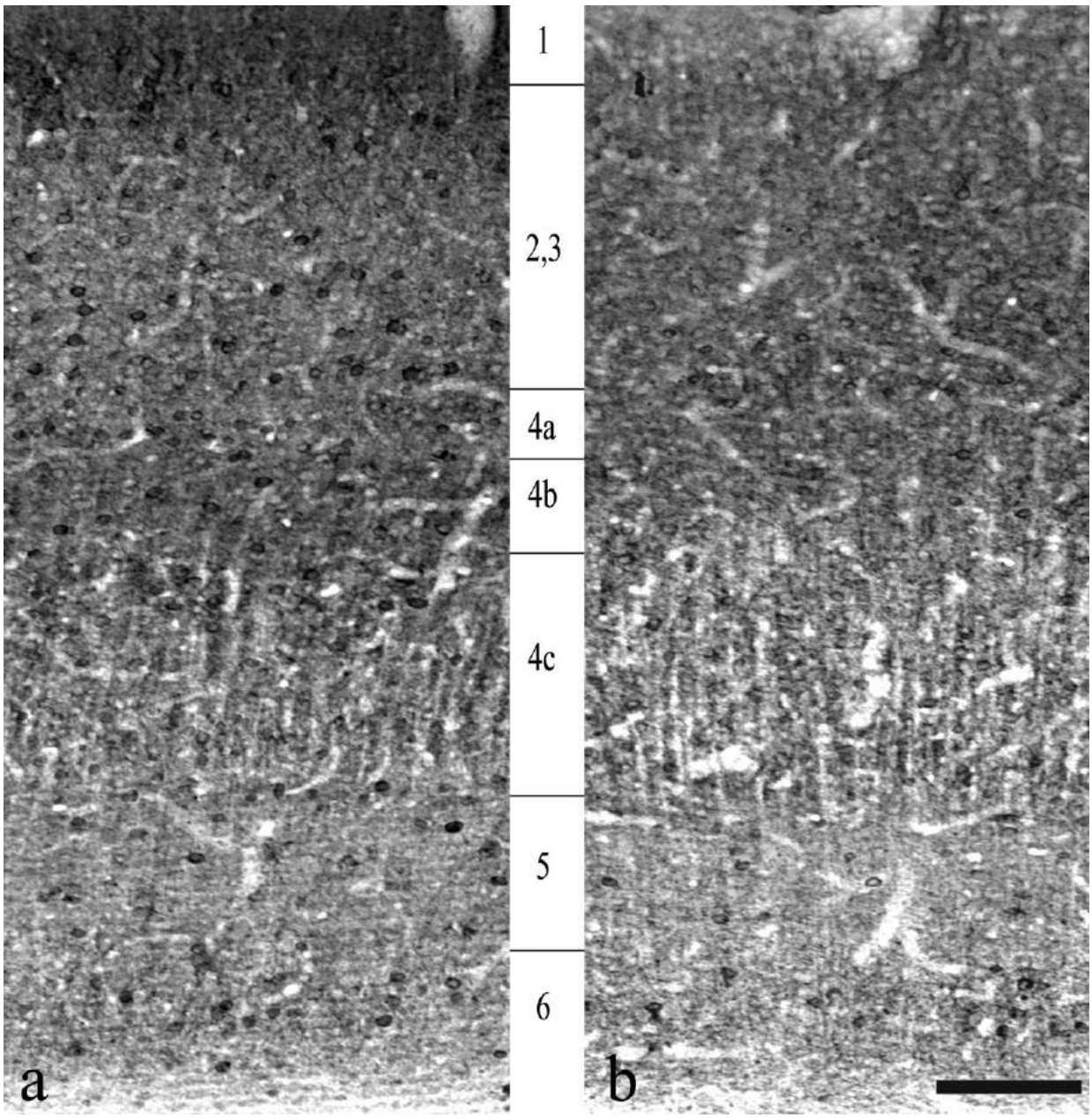

Figure 3.
Laminar distribution of Kv3.1b- and Kv3.2-ir. Photomicrographs of macaque V1, processed to show immunoreactivity for Kv3.1b **(a)** and Kv3.2 **(b)** channel subunits. Black bars between each micrograph show laminar boundaries. Kv3.1b-ir neurons (a) appear evenly distributed throughout layers 2–6. Diffuse staining of the neuropil is also present in all layers, but is stronger in layers 1–4c. Kv3.2-ir neurons (b) are also found in all layers, but appear more prominent in layers 5 and 6 in this low-power micrograph as a result of fainter neuropil staining in these layers. Scale bar = 50 μm.

Kv3.2-ir somata were expressed most frequently in neurons in layer 4, with a lower density in layers 2/3, 5, and 6 (Fig. 7, Table 2).

A comparison of the distributions of Kv3.1b- and Kv3.2-ir somata shows that Kv3.1b-ir neurons are significantly more numerous in layers 2/3 ($P < 0.01$; Student's *t*-test) (Fig. 7, Table 2). In layer 4a, however, there are more Kv3.2-ir somata than Kv3.1b-ir somata ($P < 0.05$; Student's *t*-test). Furthermore, in layer 4c Kv3.2-ir neurons (35,400/mm^3) outnumber GABAergic neurons (27,000/mm^3).

Comparison between CO rich and sparse regions—blobs and interblobs

Cortical tissue processed for cytochrome oxidase (CO), a mitochondrial enzyme that indicates levels of metabolic activity, shows identifiable laminar boundaries (Wong-Riley,

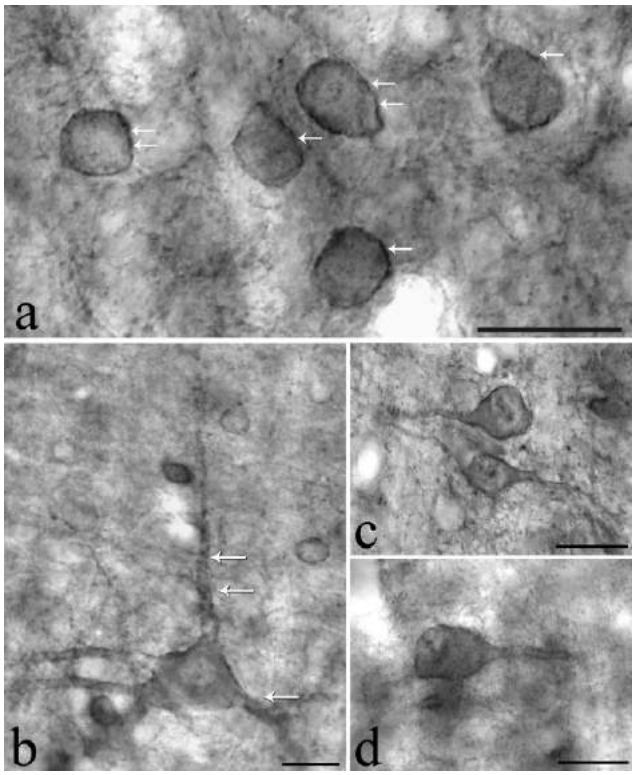

Figure 4.
Immunoreactivity for Kv3.1b in V1. Tissue sections of macaque V1 processed for Kv3.1b-ir show many labeled somata in all layers. The somatic labeling usually consists of faint intracellular labeling accompanied by an intense ring of immunoreactivity at the perimeter of the cell body **(a,** thin arrows), perhaps indicating plasmalemmal localization of the Kv3.1b protein. In many Kv3.1b-ir neurons there is little or no labeling of the major proximal axonal or dendritic processes. Meynert cells **(b)**, a morphologically distinct class of neurons with large somata that reside near the border between layers 5 and 6, show Kv3.1b-ir of their somata as well as their proximal apical and basal dendrites (b, thick arrows). Similarly, neurons in layer 4b with large, horizontally elongated cell bodies and a bipolar morphology express Kv3.1b in their somata and proximal dendrites **(c,d)**. Neither Meynert cells nor 4b bipolars show Kv3.2-ir (not shown). Scale bars = 20 μm.

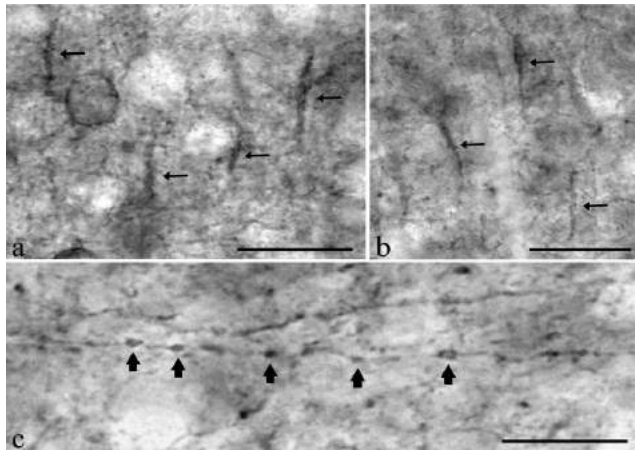

Figure 5.
Nonsomatic Kv3.1b-ir. Kv3.1b-ir is occasionally observed in neuronal processes. For example, Kv3.1b is expressed in the upper part of layer 2, in the vertically oriented dendrites (extending perpendicular to layer 1) (thin arrows in **a,b)**. Kv3.1b-ir is also occasionally observed in axons **(c)**, which can be identified by the presence of varicosities (fat arrows). Scale bars = 20 μm in a,b; 10 μm in c.

1979; Rockland and Lund, 1983). In macaque V1, CO histochemistry also reveals clearly differentiated reactive and nonreactive patches in layers 2/3, which are often called blobs and interblobs, respectively.

Somatic and neuropil immunoreactivity for Kv3.1b and Kv3.2 was examined in areas of tissue corresponding to CO-rich patches, or blobs, in layers 2/3, and compared to the immunoreactivity in areas of tissue corresponding to interblob regions. Cell body staining was quantified by stereological methods. Data were collected from 99 disectors within blobs and 108 disectors in interblobs for Kv3.1b and from 72 disectors in each of the blob and interblob regions for the Kv3.2 subunit. There was no trend toward differences in the density of Kv3-ir neurons between the blob and interblob regions. Additionally, the intensity of neuropil staining did not vary in relation to CO blob–interblob staining patterns.

Dual Kv3.1b/GABA-ir profile

In the rodent neocortex all Kv3.1b-ir neurons are GABAergic (Chow et al., 1999). If there was a close correspondence between rodent and macaque brain with respect to Kv3.1b channel subunit expression it would be predicted that all Kv3.1b-ir neurons in macaque neocortex would also be GABA-ir. However, the stereological data described above showed that Kv3.1b-ir neurons outnumber GABAergic interneurons in layers 4b and 4c of cortical area V1. It was also observed by ourselves and another group (Ichinohe et al., 2004) that glutamatergic Meynert cells show Kv3.1b-ir. To attempt to address this issue more directly, immunofluorescent dual-labeling techniques were used to determine the extent to which Kv3.1b subunits and GABA are expressed by the same cells.

Between 71% (Corrected 379 of 548; Raw 521 of 753 neurons; layers 5 and 6) and 76% (Corrected 462 of 611; Raw 634 of 851 neurons; layers 1–4) of Kv3.1b-ir somata were also GABA-ir (Table 3). Among the neurons that were Kv3.1b-ir but did not express GABA, we observed neurons in layer 4b with horizontally elongated somata, suggestive of a bipolar morphology (Fig. 8a,e). The Meynert cells described in the sections above were also identifiable in these dual-immunolabeled sections and again showed distinct labeling for Kv3.1b but not GABA. Additionally, we occasionally observed GABA-ir puncta surrounding Kv3.1b single-labeled neurons; these may be perisomatic baskets of GABAergic release sites (Fig. 8b,d,f).

A higher proportion of GABAergic interneurons express Kv3.1b in macaque V1 than in rodent neocortex. Only 50% of cortical GABAergic interneurons in rodents express Kv3.1b (Chow et al., 1999), whereas in the macaque V1 this proportion is much larger; ≈85% of GABAergic (1,121 of 1,313) interneurons are Kv3.1b-ir (Table 3).

Dual Kv3.2/GABA-ir profile

Similar to Kv3.1b, Kv3.2 is exclusively expressed in GABAergic interneurons in the rodent neocortex and only 40% of GABAergic neurons are Kv3.2-ir (Chow et al., 1999). In comparison, in macaque V1, 74% (Corrected 203 of 260; Raw 279 of 344 neurons; layers 1–4) and 80% (Corrected 98 of 122;

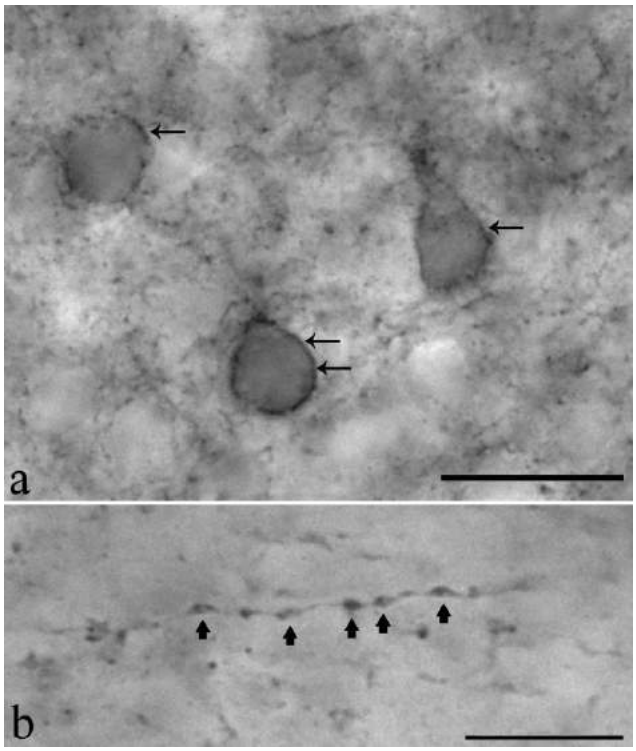

Figure 6.
Immunoreactivity for Kv3.2 in macaque V1. Tissue sections of macaque V1 processed for Kv3.2-ir show many labeled somata **(a)** in all layers, although labeled neurons in layers 2–4 are difficult to distinguish at low power as a result of prominent neuropil-immunoreactivity (see Fig. 3). Similar to Kv3.1b, somatic labeling for Kv3.2 usually consists of an intense ring of immunoreactivity around the cell body (thin arrows), perhaps indicating plasmalemmal localization of the Kv3.2 protein. In most Kv3.2-ir neurons there is little or no labeling of the major proximal axonal or dendritic processes; however, Kv3.2 is occasionally expressed in axons **(b)**. These axons are not clearly associated with nearby somata. Note the clearly distinguishable varicosities (thick arrows), which show the typical axonal "beads on a string" appearance. Scale bars = 20 μm in a; 10 μm in b.

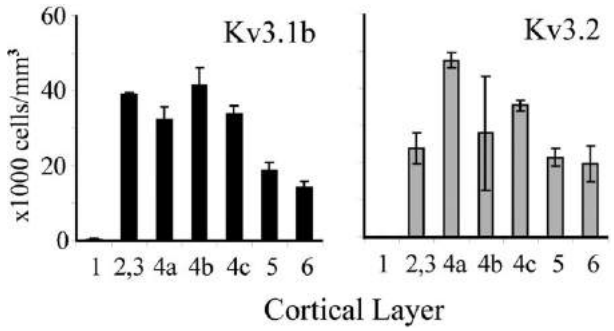

Figure 7.
Number ($\times 10^3$) of Kv3.1b- and Kv3.2-ir neurons per cubic millimeter of tissue in macaque V1. Means and SEM values (n = 3) are given for each cortical layer. These values were obtained by the optical disector method.

Raw 134 of 161 neurons; layers 5 and 6) of Kv3.2-ir neurons were GABAergic (Table 3, Fig. 9). It was also found that ≈89% of GABA-ir (Corrected 725 of 860; Raw 960 of 1,182) interneurons expressed Kv3.2.

TABLE 2. Number ($x10^3$) of Kv3.1b-, Kv3.2-, and GABA-ir Neurons per Cubic Millimeter of Tissue in Macaque V1

Layers	N(v)[1]Kv3.1b-ir neurons per mm^3	N(v)[1]Kv3.2-ir neurons per mm^3	N(v)[1]GABA-ir neurons per mm^3
1	.367 ± 0.141	0.00 ± 0	11.5 ± 1.6
2,3	39 ± 0.624	23.9 ± 4.31	28.2 ± 1.26
4a	32.1 ± 3.73	47.5 ± 2.05	44.5 ± 20.0
4b	41.4 ± 4.86	28.0 ± 15.3	20.4 ± 3.68
4c	33.8 ± 2.14	35.4 ± 1.48	27.0 ± 4.5
5	18.7 ± 2.15	21.4 ± 2.33	22.3 ± 2.17
6	14.2 ± 1.66	19.6 ± 4.88	16.5 ± 12.05
1-6	25.67 ± 1.24	25.08 ± 3.67	23.6 ± 2.7

[1]Numerical density, or N(v), is the number ($x10^3$) of neurons per cubic millimeter of tissue. Means and SEM values (n = 3) are given for Kv3-ir neurons.
Means and SEM values (n = 4) of GABA-ir cells from counts from tissue processed for GABA-immunoreactivity are adapted from Beaulieu et al. (1992). Beaulieu et al. (1992) collected these data using the optical disector method.

Dual Kv3.1b/PV-ir profile

Dual-labeling techniques were used to determine the extent to which Kv3.1b subunits are expressed by neurons immunoreactive for PV, a calcium-binding protein that is often used as an anatomical marker for FS GABAergic interneurons (Kawaguchi and Kubota, 1993; Kawaguchi and Kubota, 1997; Cauli et al., 1997). Many neurons clearly showed dual labeling for Kv3.1b and PV (Fig. 10). However, Kv3.1b and PV were not always co-expressed (Fig. 11). In fact, only 78% of Kv3.1b-ir (Corrected 506 of 651; Raw 593 of 767) neurons expressed PV (Table 3, Figs. 11a, 12), and only 89% of PV-ir neurons were Kv3.1b-ir (Table 3, Fig. 11e).

Kv3/PV dual-labeled tissue was also informative of the subcellular localization of Kv3.1b. Kv3.1b punctate labeling was frequently observed and occasionally several puncta clustered around the periphery of a labeled or unlabeled soma, appearing to be in close apposition to that soma. These puncta collectively resembled perisomatic baskets (Fig. 11c,i).

Dual Kv3.2/PV-ir profile

About 75% of Kv3.2-ir (Corrected 763 of 1,011; Raw 895 of 1,159) neurons also expressed PV in layers 1–4, and comparably, 76% of Kv3.2-ir (Corrected 598 of 784; Raw 701 of 899) neurons expressed PV in layers 5 and 6 (Table 3; Fig. 13). Of the PV-ir neurons, 94% were Kv3.2-ir (Table 3).

Dual Kv3.1b/CB-ir profile

PV- and CB-ir inhibitory neurons comprise almost entirely nonoverlapping populations in V1 of the macaque. Examining expression across these two populations enables an assessment of >86% of the inhibitory population in this region. The remaining 14% of GABAergic neurons include CR-ir neurons (a population that partially overlaps the CB-ir population) and a small population of cells that do not express any of these calcium-binding proteins. The CB-ir population is heterogeneous, consisting of two groups of neurons that are distinguished by the darkness of their immunostaining. Darkly stained CB-ir neurons are primarily expressed in layers 2, 4b, and 5, whereas faint CB-ir neurons are expressed in all layers of cortex (Van Brederode et al., 1990; Disney and Aoki, 2008). All darkly stained CB-ir neurons are GABAergic (Van Brederode et al., 1990); however, it is likely that some of the lightly stained CB-ir neurons are non-GABAergic (Van Brederode et al., 1990; Disney and Aoki, 2008). Since CB was used as a marker for GABAergic interneurons in this study, only counts of darkly stained CB-ir neurons are reported.

TABLE 3. Coexpression of GABA and Ca^{2+}-binding Proteins with Kv3.1b or Kv3.2 Channel Subunits in Macaque V1

	GABA [%(n)]	PV [%(n)]	Dark CB [%(n)]	Kv3.1b [%(n)]	Kv3.2 [%(n)]
Kv3.1b					
1-4	75.84 ± 2.16 (462/611)	80.06 ± 3.16 (359/455)	14.71 ± 1.87 (268/1817)		
5-6	70.6 ± 1.43 (379/548)	75.01 ± 3.48 (147/196)	7.35 ± 1.77 (114/1573)		
Kv3.2					
1-4	74.26 ± 5.30 (203/260)	75.46 ± 3.89 (763/1011)	11.70 ± 0.29 (274/2331)		
5-6	80.52 ± 1.30 (98/122)	76.25 ± 2.01 (598/784)	9.76 ± 0.855 (174/1806)		
GABA				84.01 ± 2.28 (805/956)	88.85 ± 7.42 (725/860)
PV				88.89 ± 1.73 (1147/1292)	93.63 ± 1.15 (1392/1478)
Dark CB					
1-4				60.36 ± 18.80 (265/423)	48.78 + 2.50 (312/632)
5-6				34.04 ± 4.55 (113/349)	44.01 ± 3.83 (177/404)

Data are mean percentages ± SEM values calculated from Abercrombie corrected neuronal counts (corrected total counts in parentheses – note that percentages given are averages across animals and were not calculated from the total counts presented in this table). For Kv3/PV, n = 3. For Kv3/GABA and Kv3/CB, n = 2 animals. Although counting cells from confocal micrographs was the preferred method of data collection, the counting method was adjusted by dataset to correct for biases produced by specific antibody staining patterns (see Materials and Methods). When PV- and CB-ir neurons were the base populations that were counted, an epifluorescent microscope was used to examine each labeled cell through all depths of the tissue by manually moving through the z-axis in both fluorescent channels. When GABA-ir neurons were the base population, the same method was adopted but only at either surface of the tissue section. When Kv3.1b- and Kv3.2-ir neurons were the base populations in tissue processed for dual-labeling with PV or GABA, Kv3 single- and dual-labeled neurons were counted from confocal photomicrographs. When Kv3-ir neurons were the base populations in tissue processed for dual-labeling with CB, Kv3 single- and dual-labeled neurons were counted in epifluorescence.

In layers 1–4, 15% (Corrected 268 of 1,817; Raw 312 of 2,140) of Kv3.1b-ir neurons expressed CB, whereas in layers 5 and 6, only 7% of Kv3.1b-ir (Corrected 114 of 1,573; Raw 133 of 1,853) neurons expressed CB (Table 3, Fig. 14). About 60% of the CB-ir neurons in layers 1–4 expressed Kv3.1b, while only 34% of CB-ir neurons in layers 5 and 6 were Kv3.1b-ir (Table 3).

Dual Kv3.2/CB-ir profile

A small proportion of Kv3.2-ir neurons also expressed CB: 12% in layers 1–4 (Corrected 274 of 2,331; Raw 319 of 2,673) and 10% (Corrected 174 of 1,806; Raw 203 of 2,071) in layers 5 and 6 (Table 3). These dual-labeled cells represent ≈49% of the CB population in layers 1–4 and 44% in layers 5 and 6 (Table 3).

Kv3.2/CB dual-labeled tissue was again informative of the subcellular localization of Kv3.2. In particular, we frequently observed Kv3.2 punctate labeling, including clustered puncta around CB-ir neurons (data not shown).

Dual in situ hybridization/immunocytochemistry (ISH/ICC)

It is possible that a failure to detect all of the GABA-expressing neurons using the GABA antibody could account for some of our results. To examine this possibility we performed experiments in which in situ hybridization to detect mRNAs for the 67 kD form of glutamic acid decarboxylase (GAD67) or for the alpha subunit of calcium/calmodulin-dependent protein kinase A (CaMKIIα) was combined with immunocytochemistry to visualize expression of the Kv3.1b subunit. GAD67 is expressed only in GABAergic neurons and CaMKIIα is expressed only in principal cells (but not in all principal cells: Benson et al., 1992; Jones et al., 1994; Liu and Jones, 1996). While most Kv3.1b-ir neurons hybridized for GAD67 mRNA, some showed no hybridization signal (Fig. 15). Conversely, while most Kv3.1b-ir neurons did not show CaMKIIα hybridization, there were a number of cells that were clearly dual-labeled for Kv3.1b protein and for CaMKIIα mRNA (Fig. 16).

DISCUSSION

There are two major findings in this study. First, a proportion of Kv3-ir neurons in macaque V1 are putatively excitatory. The evidence for this is 5-fold; some Kv3.1b-ir neurons are easily identifiable (morphologically) as being glutamatergic neurons (e.g., the Meynert cells and the horizontal bipolar cells in layer 4b). Additionally, the stereological counts of the numbers of Kv3-ir neurons in each cortical layer and their comparison with the density of GABAergic neurons in each layer reported by Beaulieu et al. (1992; their table 2) show that Kv3.1b-ir neurons outnumber GABA-ir neurons in some layers of macaque V1. Our immunofluorescent dual-labeling studies in which tissue was processed for Kv3- and GABA-ir also reveal that only 75% of Kv3-ir neurons express GABA (Table 3). This result is supported by the dual ISH/ICC showing that there are Kv3.1b-ir cells that do not contain GAD67 mRNA (GAD67 being the more abundant form in macaque V1, showing active expression in 96% of GABA-ir neurons; Hendrickson et al., 1994). Finally, we provide positive evidence for the existence of Kv3.1b-expressing principal cells with the demonstrated existence of Kv3.1b-ir neurons that show a hybridization signal for CaMKIIα mRNA.

The second major finding of this study is that Kv3 channel subunits are expressed differently across subpopulations of GABAergic interneurons in macaque V1, compared to the rodent neocortex. For example, in the rodent neocortex ≈50% of GABA-ir neurons are also Kv3.1b-ir and all of these Kv3.1-ir neurons express PV (Chow et al., 1999). In macaque V1, however, 84% of GABA-ir neurons are Kv3.1b-ir. Given that only 74% of GABA-ir neurons in V1 are PV-ir (Van Brederode et al., 1990), this implies that some non-PV neurons also express Kv3.1 subunits. This latter conclusion is supported by the observation that between 7% (layers 5 and 6) and 15% (layers 1–4) of Kv3.1-ir neurons express CB. It has been reported previously that neurons expressing both CB and PV are extremely rare in macaque V1 (Van Brederode et al., 1990).

It is important to point out, however, that the results of this study also show that there are substantial similarities between rodents and macaques in the populations of Kv3.1b- and Kv3.2-expressing neocortical neurons. As in the rodent, in macaque V1 the vast majority of PV-ir neurons (perhaps all PV-ir neurons) express a subunit from the Kv3 channel family, confirming immunocytochemically the physiological observation from experiments using the in vitro slice preparation of monkey prefrontal cortex that most PV-ir neurons are fast-spiking (Zaitsev et al., 2005).

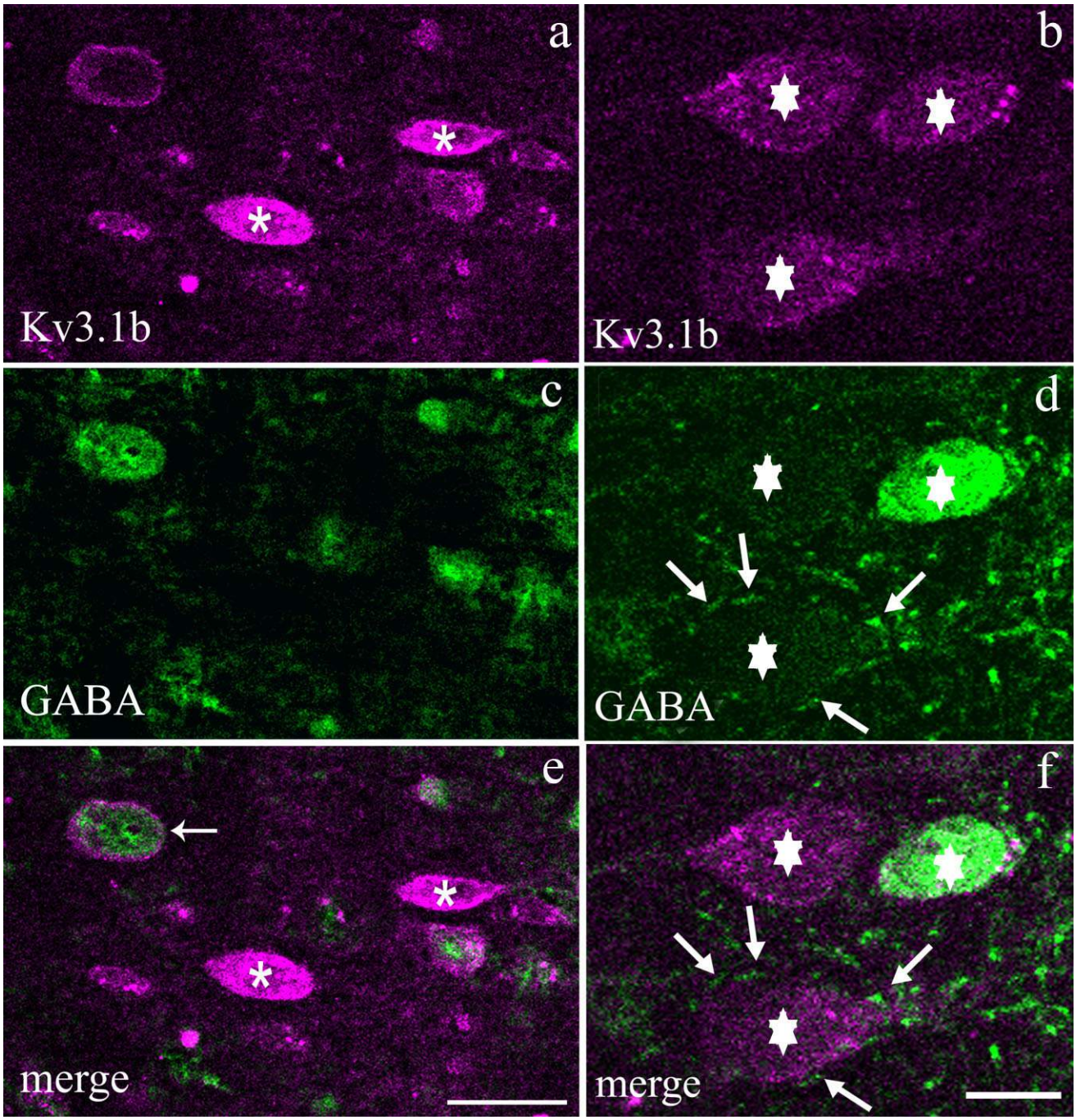

Figure 8.
Some Kv3.1b-ir neurons are non-GABAergic, including neurons in layer 4b. Confocal photomicrographs of tissue processed by dual immunofluorescence to show Kv3.1b **(a,b)** and GABA **(c,d)** immunoreactivity. The images in the left column (a,c,**e),** were taken from layer 4b and in the isolated "red" channel (here false-colored magenta, a) several Kv3.1b-ir somata are visible, along with diffuse neuropil staining. Similar to our observations in tissue processed using the immunoperoxidase method, several of the Kv3.1b-ir neurons in layer 4b have large, elongated somata (asterisks; see Fig. 4c,d). The isolated green channel (c) shows labeling of GABA-ir somata, and some neuropil labeling. The merged image (e) shows one Kv3.1b/GABA dual-labeled neuron (thin arrow; e), whereas the two putative bipolar cells that express Kv3.1b do not express GABA (asterisks; a,e). The images in the right column (b,d,**f)** show a dual-immunofluorescence image from layer 4c with three Kv3.1b-ir neurons (stars; b,d,f), one of which is dual-labeled for GABA (d). Another of the Kv3.1b-ir neurons is surrounded by closely apposed varicosities which are GABA-ir (thick arrows; d,f). These varicosities may represent the puncta of a GABAergic perisomatic basket. Scale bar = 20 μm in e (applies to a,c); 10 μm in f (applies to b,d).

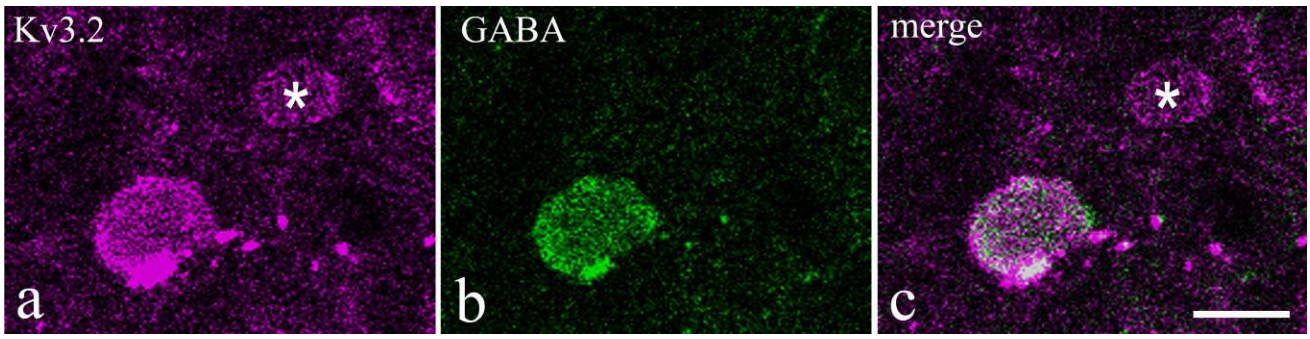

Figure 9.
Some Kv3.2-ir neurons are non-GABAergic. This dual-immunofluorescence image from layer 4c shows labeling for Kv3.2 **(a)** and GABA **(b)**. The "red" channel (colored magenta in this figure) shows somatic labeling of two Kv3.2-ir neurons and diffuse neuropil labeling. Comparison with the middle panel (b) and the merged image **(c)** shows that one of these Kv3.2-ir neurons (asterisk) does not express GABA. Scale bar = 10 μm.

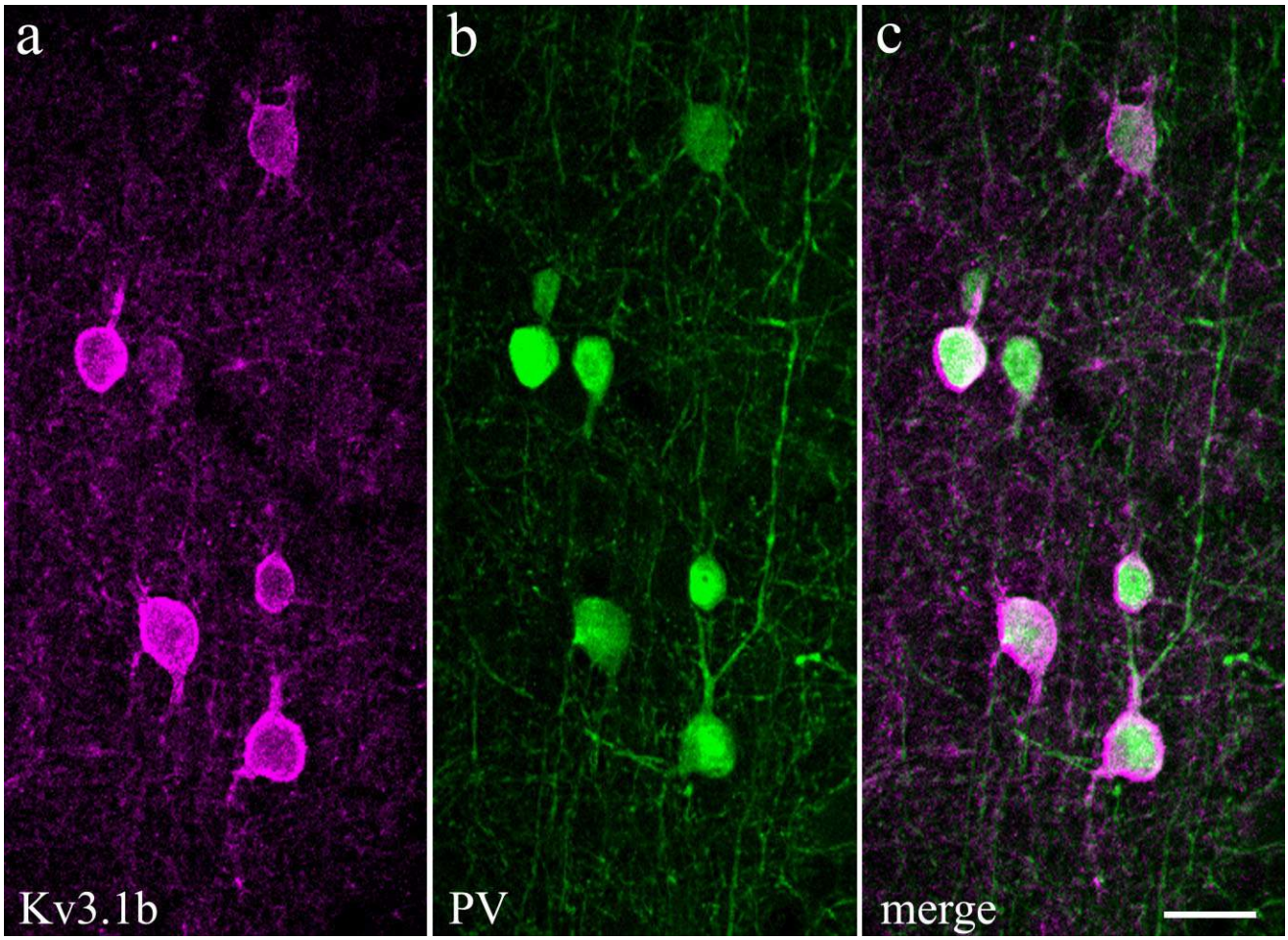

Figure 10.
Most PV-ir neurons express Kv3.1b. This dual immunofluorescence image taken from layer 2/3 of V1 shows that Kv3.1b **(a)** and PV **(b)** are frequently coexpressed in the same neurons. All of the somata shown in this image are immunoreactive for both Kv3.1b and PV (i.e., all somata appear in both channels; a,b) and look white in the merged image **(c)**. This image also shows that the subcellular localization of the two antigens differs. Kv3.1b labeling (a) is most intense at the somatic periphery, and usually includes only very proximal axonal or dendritic processes. PV labeling (b), conversely, appears cytosolic and often includes dendrites and axons as well as the cell somata. Scale bar = 20 μm.

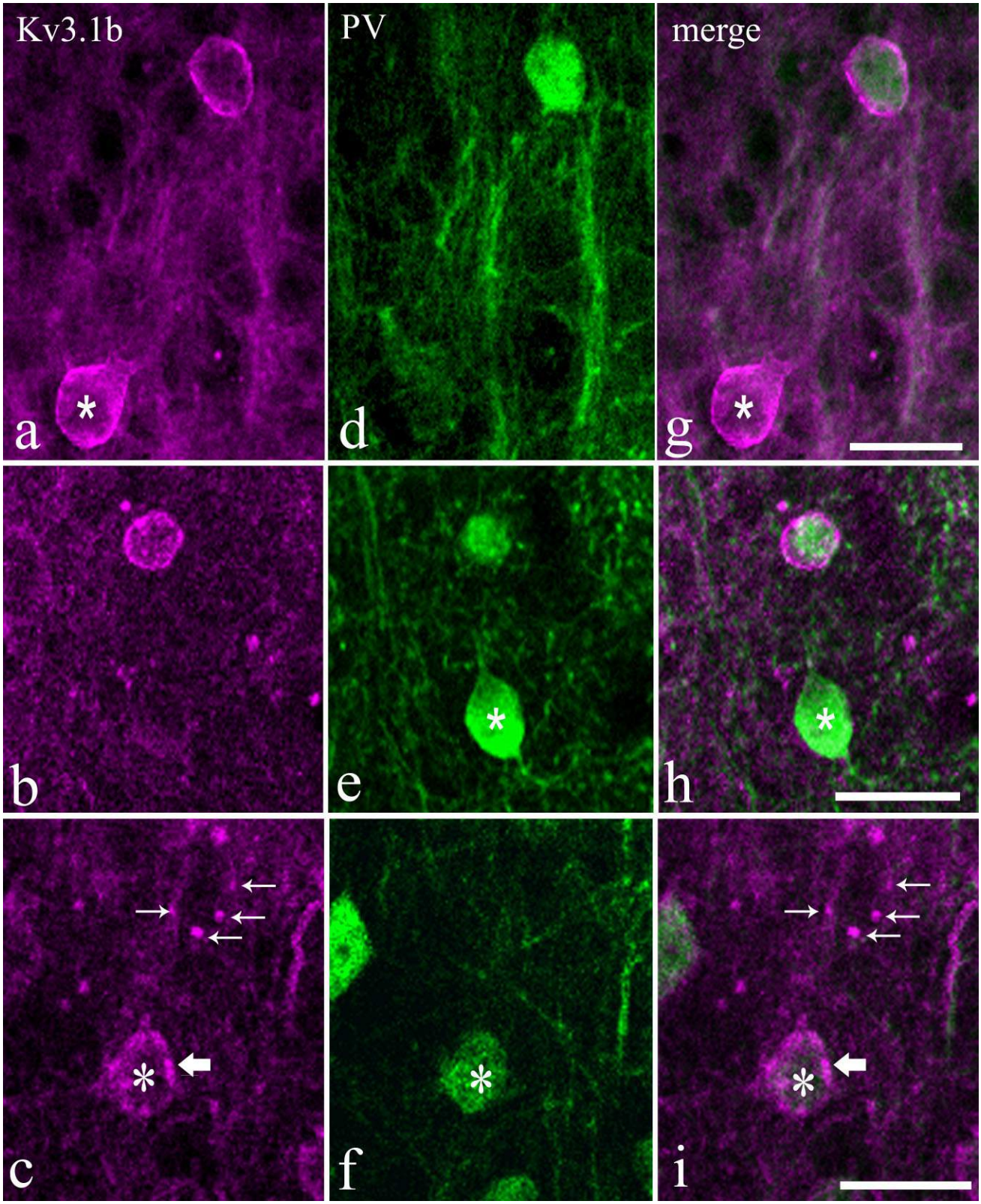

Figure 11.
Kv3.1b and PV do not always colabel somata in macaque V1. The top row **(a,d,g)** shows a dual immunofluorescence image taken from layer 4c of V1. The isolated "red" channel (a) shows two Kv3.1b-ir somata, as well as neuropil labeling. The green channel (d) shows PV-ir in one soma as well as in the neuropil. The merged image (g) shows that one of the Kv3.1b-ir neurons is dual-labeled, while one neuron (asterisk; a,g) expresses Kv3.1b but not PV. In the middle row **(b,e,h)**, a dual immunofluorescence image (also from layer 4c) shows a PV-ir neuron (asterisk; e,h) that does not express the Kv3.1b channel subunit. The merged (h) and separate (b,e) images show one neuron dual-labeled for Kv3.1b (b) and PV (e), and one neuron that expresses PV (asterisk; e,h). The bottom row **(c,f,i)** shows labeling for Kv3.1b (c) and PV (f). In the "red" (c) and merged (i) channels, Kv3.1b-ir puncta can be seen (thin and fat arrows; c,i). The thin arrows indicate puncta which appear to be clustered close to a soma that is neither Kv3.1b- (c) nor PV-ir (f). These clustered puncta are suggestive of a Kv3.1b-ir perisomatic axonal basket. The puncta indicated by the fat arrow (c,i) are more difficult to clearly interpret as axonal because the postsynaptic neuron (asterisk; c,f,i) is immunoreactive for Kv3.1b. These puncta could equally well represent axonal varicosities or clusters of Kv3.1b subunits on the postsynaptic membrane. Scale bars = 20 μm.

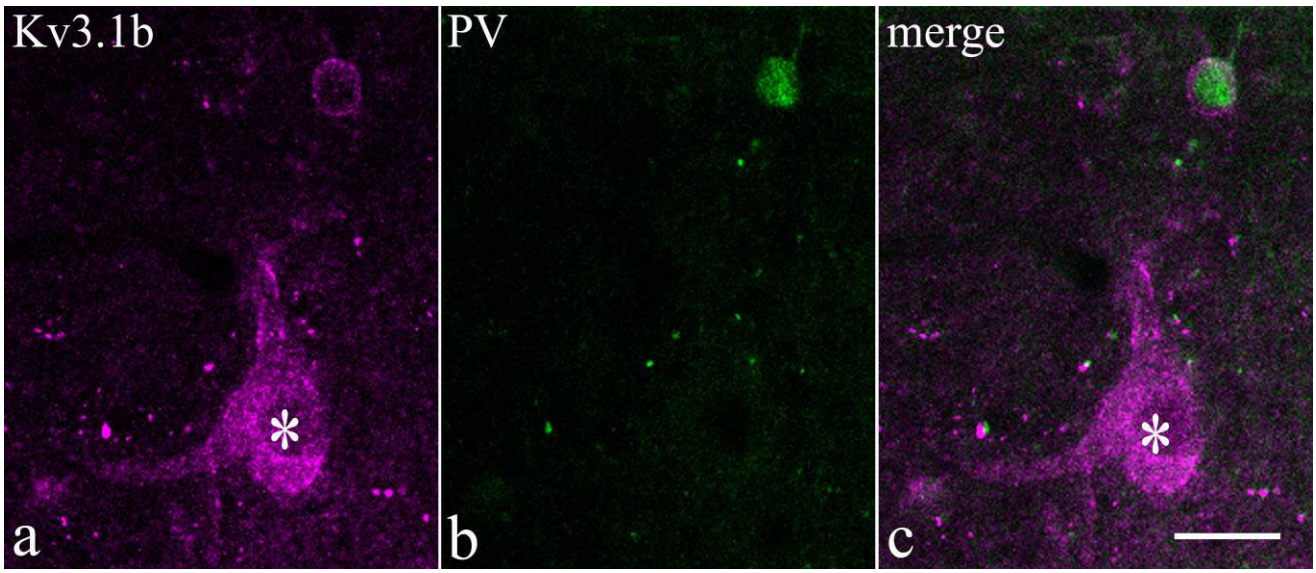

Figure 12.
Meynert cells express Kv3.1b but not PV. In this dual immunofluorescent image of neurons in layer 6 the "red" channel **(a)** shows Kv3.1b-ir in two layer 6 neurons, including a Meynert cell (asterisk). The green channel **(b)** shows one neuron is immunopositive for PV. The merged image **(c)** shows that the Meynert cell (asterisk) expresses Kv3.1b but not PV. Scale bars = 20 μm.

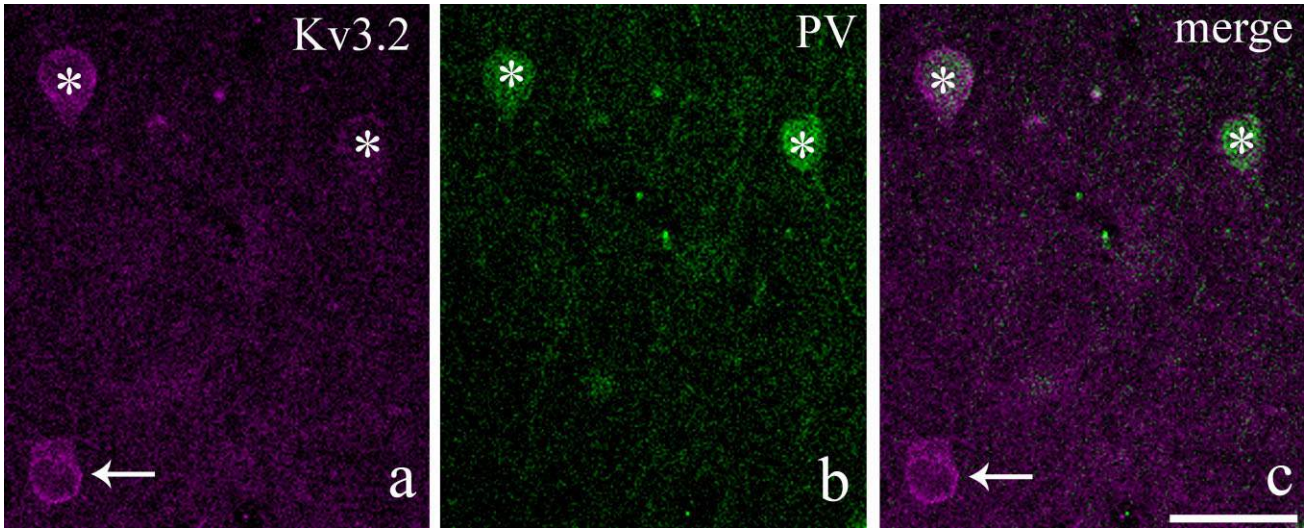

Figure 13.
Some Kv3.2-ir neurons do not express PV. In this dual immunofluorescence image of neurons in layers 2/3 the "red" channel **(a)** shows three Kv3.2-ir somata. The green channel **(b)** shows two PV-ir neurons. The merged image **(c)** shows that both of these PV-ir neurons are dual-labeled for Kv3.2 and PV (asterisks), and the other neuron expressed Kv3.2 but not PV (arrow). Scale bar = 20 μm.

Expression of Kv3.1b and Kv3.2 in putatively excitatory populations

Stereological counts of neurons expressing Kv3.1b show that this population is greater than the total population of GABAergic neurons in layers 2/3, 4b, and 4c (Table 2). Across these layers, 25% of Kv3.1b- and Kv3.2-ir neurons are non-GABAergic in macaque V1 (Table 3). This is in contrast to data from the rodent neocortex, which show that >99% of Kv3.1b-ir and 96–98% of Kv3.2-ir neurons are GABAergic (Chow et al., 1999).

The validity of the comparison between the size of the GABA-ir population and the sizes of the Kv3.1b-ir and Kv3.2-ir populations depends heavily on successful antigen detection in the tissue of interest. There exists the possibility in any immunocytochemical study that some members of the population of interest are not detected by the methods chosen. In the present study, detection of GABA is particularly important as it is assumed that all cells not immunoreactive for GABA are, in fact, glutamatergic. This assumption is supported by previous studies that have shown that, in macaque V1, the

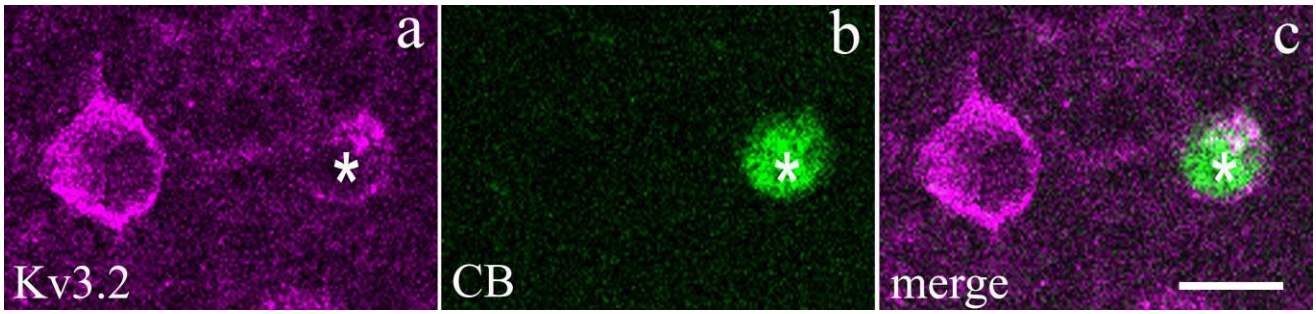

Figure 14.
Some Kv3.1b-ir neurons in layers 1–4 express CB. This dual immunofluorescence image of neurons in layer 2/3 shows two Kv3.1b-ir somata **(a)** one of which is also CB-ir **(b,c;** asterisk). Scale bar = 20 μm.

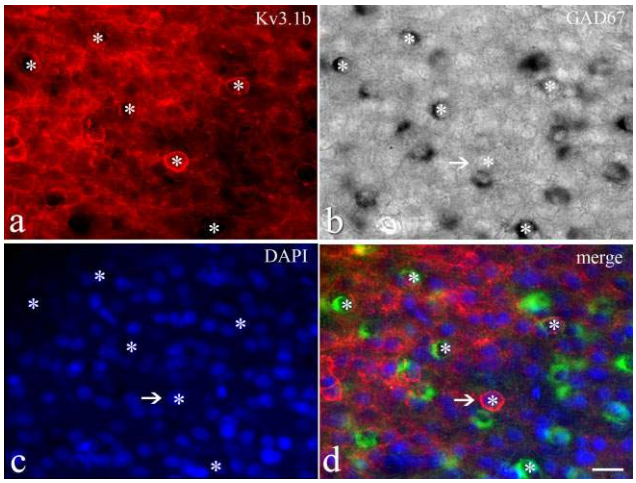

Figure 15.
Some Kv3.1b-ir neurons do not express GAD67 mRNA. These panels show a region from layer 3 of tissue dual-labeled for Kv3.1b protein (by immunocytochemistry) and for GAD67 mRNA (by in situ hybridization). In **(a)** a number of Kv3.1b-ir neurons can be seen (some of which have been marked with asterisks for comparison with other panels). In **(b)** the hybridization signal for the same region of tissue shows that while most of these neurons also express GAD67, there is one neuron that does not (arrow). Given that it has been shown that GAD67 is probably expressed in all inhibitory neurons in macaque V1 (Hendrickson et al., 1994), and given that glycine is not a primary neurotransmitter in this region, the GAD67-negative cell is likely to be excitatory. The DAPI stain in **(c)** confirms that these immunoreactive cells are all neurons. In the three-channel merged image **(d)** the in situ signal has been false-colored green and inverted. Scale bar = 20 μm.

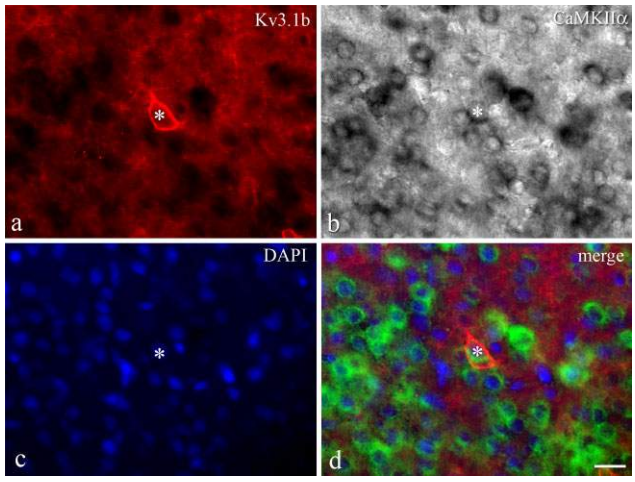

Figure 16.
CaMKIIα gene expression by a Kv3.1b-ir neuron. These micrographs show a neuron from layer 2 that is immunoreactive for Kv3.1b protein (asterisk; **a).** This same neuron also expresses mRNA for CaMKIIα (asterisk; **b),** which has previously been shown to be expressed only by excitatory neurons in the macaque neocortex (Jones et al., 1994). This neuron's nucleus appears in the DAPI stain **(c)** and the soma also appears to have a pyramidal morphology, further suggesting that it is an excitatory neuron. In the merged image **(d)** the in situ hybridization signal has been inverted and false-colored (green). Scale bar = 20 μm.

primary neurotransmitter substance for at least 95% of neurons is either GABA or glutamate (for review, see DeFelipe, 1993). While there is no absolute measure of the sensitivity of the GABA detection achieved in this (or any) large-scale quantitative study, there is evidence that our detection is likely to be as good as that achieved in other immunocytochemical studies with which our data are here compared (all of which used antibodies against GABA to identify inhibitory neocortical neurons). In comparing the counts we obtained using immunofluorescence with those obtained by Hendry et al. (1987) using the highly sensitive immunoperoxidase method we found that our detection of GABA neurons was comparable to that study (see Materials and Methods, GABA-ir Neurons). Additionally, we confirmed that our immunofluorescence protocol enabled us to correctly identify >98% of CB and PV neurons as GABAergic (see Materials and Methods, GABA-ir Neurons) and we showed that using in situ hybridization for GAD67 in place of immunological detection of GABA still results in single-labeled Kv3.1b-ir neurons. Finally, our dual ISH/ICC results also provide positive evidence for the existence of excitatory neurons that express Kv3.1b potassium channel subunits because in both rodents and macaque neocortex, CaMKIIα is only expressed in glutamatergic neurons (but is not expressed in all glutamatergic neurons: Benson et al., 1992; Jones et al., 1994: Liu and Jones, 1996). Given that glycine is not a neocortical inhibitory neurotransmitter (Rajendra et al., 1997), these ISH/ICC results, combined with the stereological and dual-immunofluorescence data and the controls for GABA detection, support a conclusion that the majority of the non-GABA-ir, Kv3-expressing neurons we observed in V1 are in fact cortical excitatory cells.

Although it was difficult to classify most of the neuronal types that were Kv3-ir but not GABA-ir by their axonal or dendritic morphology (due to incomplete staining of the cell arbors) there were two groups of these Kv3-expressing, putatively excitatory neurons that could be morphologically classified. One of these groups included neurons that had large, elongated cell bodies (Figs. 4c,d, 8a). These cells fit the description of spiny stellate cells with horizontally extended dendritic fields in layer 4b (which in macaque V1 is not thalamic-recipient—layer 4b receives ascending input from layer 4c), as observed in Golgi preparations (Lund, 1973). The other putatively excitatory neurons that were found in this study to be Kv3.1b-ir were Meynert cells in layers 5/6 (Fig. 12). Ichinohe et al. (2004) previously reported that Meynert cells express Kv3.1b and also express the calcium-binding protein PV. Although our observations confirm the expression of Kv3.1b in these neurons (Fig. 4b), our Kv3.1b/PV dual-labeling showed that none of these Meynert cells expressed PV (Fig. 12). Expression of PV by Meynert cells has not been reported in other large-scale studies of calcium-binding protein immunoreactivity in macaque V1 (see, for example, Van Brederode et al., 1990; DeFelipe et al., 1999; Disney and Aoki, 2008). Examining the figures presented by Ichinohe et al. (2004) indicates that the difference between the conclusions in that report and those of the present study, with respect to PV-ir of Meynert cells, is certainly the result of the different counting criteria used in the two studies. The counting method adopted in the current study was consciously conservative in dealing with punctate perisomatic labeling because the confocal microscope is inadequate to resolve pre- versus postsynaptic localization of immunoreactivity.

Role of Kv3 channels in excitatory neurons

While excitatory neurons in the neocortex of rodents do not express Kv3.1b channels, in subcortical structures of the auditory pathway, both excitatory neurons in the cochlear nucleus and projecting inhibitory neurons in the medial nucleus of the trapezoid body (MNTB) express Kv3.1b (Perney et al., 1992; Weiser et al., 1994; Perney and Kaczmarek, 1997; Wang et al., 1998; Elezgarai et al., 2003). Within the MNTB, Kv3.1b is expressed along a tonotopic gradient such that the highest expression is in the medial end, which is responsible for the processing of high-frequency auditory inputs and requires the greatest degree of temporal precision (Li et al., 2001). The ability of Kv3.1b-expressing neurons to fire at high frequencies and the tonotopic expression of this channel subunit are believed to be critical for the maintenance of temporal acuity in this circuit (Wang et al., 1998; von Hehn et al., 2004; Kaczmarek et al., 2005).

In the cat and ferret cortices, chattering (Gray and McCormick, 1996; Brumberg et al., 2000) or fast rhythmic bursting (FRB; Cardin et al., 2005) cells show bursts of high-frequency firing. These physiological cell types correspond to pyramidal neurons located in the supragranular cortical layers. FRB cells have narrow (<0.5 ms) action potentials (Nowak et al., 2003; Cardin et al., 2005) that are similar in width to the action potentials of fast-spiking inhibitory interneurons (McCormick et al., 1985; Nowak et al., 2003). Since Kv3 subunit-containing potassium channels can confer a narrow spike width, it is tempting to speculate that the group of neurons that we have identified as Kv3-ir and putatively excitatory in layers 1–4 of macaque V1 (Table 2) include the chattering or FRB neurons. Chattering cells have not been reported in rodent neocortex where there are no excitatory Kv3.1b- or Kv3.2-ir neurons (Chow et al., 1999). In the cat and ferret cortices, it has been suggested that there exists a reciprocal relationship between cortical FRB neurons and thalamic interlaminar neurons, which also have narrow spikes and high burst rates, and that this relationship is involved in synchronizing high frequency thalamic and cortical oscillators that are coupled, and thus maintaining thalamocortical oscillations (Steriade, 2004). The role of Kv3 channels has been suggested as contributing to the narrow spikes and high firing rates observed in this circuit as well (Steriade, 2004).

Kv3 expression, GABAergic neurons, and calcium-binding proteins

In mouse and rat neocortex, neurons physiologically classified as FS are reported to express the calcium-binding protein PV (Kawaguchi and Kubota, 1993,Kawaguchi and Kubota, 1997; Cauli et al., 1997). As a result, PV is often used as an anatomical marker for FS neurons. Immunocytochemical studies (Chow et al., 1999) and gene expression analyses (Toledo-Rodriguez et al., 2004) indicate that Kv3.1b and Kv3.2 are coexpressed with PV in the same neurons, providing further support for the usefulness of PV as a marker for FS cells in rodents. A main finding of this study is that there are several differences in the expression patterns of the Kv3 channel subunits across subpopulations of GABAergic interneurons in macaque V1 compared to the rodent neocortex. For example, both Kv3.1b and Kv3.2 channel subunits are expressed in a larger proportion of GABAergic interneurons in macaque V1 (≈85%; Table 3) than in the rodent neocortex (40–50%; Chow et al., 1999). If, as in the mouse and rat, Kv3 potassium channels in V1 confer the narrow action potential width that is characteristic of FS cells, then there are potentially considerably more GABAergic interneurons in macaque V1 that exhibit the fast-spiking phenotype than in the rodent neocortex. Additionally, in macaque V1 we found that between 7% and 15% of Kv3.1b-ir neurons and 10% to 12% of Kv3.2 neurons express CB.

The higher proportion of GABAergic neurons that express Kv3 subunits in macaque V1 certainly in part reflects differences in the sizes of interneuron subpopulations between species. For example, since there are more PV-ir interneurons in macaque V1 and PV-ir neurons do tend to coexpress Kv3.1b (Table 3), then both PV and Kv3.1b expression will be higher in macaque V1 than in rodent neocortex. However, beyond this *larger* population of PV-ir neurons, the existence of a population of CB-ir putatively inhibitory interneurons expressing Kv3.1b channel subunits suggests that a *broader* population of inhibitory neurons in macaque V1 may be found to produce narrow spikes, possibly at high sustained firing frequencies. It is very unlikely that the CB-ir neurons are a subgroup of the PV-ir population, for two reasons: first, coexpression of CB and PV in the same neuron is rarely, if ever, seen in macaque V1 (Van Brederode et al., 1990). Second, the proportion of GABA-ir neurons that express Kv3 subunits (roughly 85%) exceeds the size of the PV-ir population (74% of all GABA-ir neurons; Van Brederode et al., 1990).

We also found that ≈10% of PV-ir neurons do not express Kv3.1b (Table 3; Figs. 11a, 12). So while there is a 1:1 relationship between PV and Kv3.1b in the rodent neocortex, this is not true in macaque V1. It is also the case that roughly 10%

of PV neurons do not express Kv3.2 subunits. In the absence of a triple-labeling study, it cannot be concluded that the 10% not expressing Kv3.1b subunits are the same 10% not expressing Kv3.2 subunits. However, if they are the same population, this would suggest that about 10% of PV cells do not express any Kv3 subunit at all (we have confirmed that Kv3.3 is not expressed in macaque V1; data not shown) and may thus differ in firing properties from the majority of PV cells, raising questions regarding the usefulness of PV as a marker for FS neurons in V1.

Our study also suggests that using PV as a marker for FS neurons in macaque V1 will miss a population of inhibitory neurons that express CB and may also be capable of FS-like behavior by virtue of their expressing Kv3 subunits. In this regard, it is interesting to note that careful inspection of Zaitsev et al.'s (2005) figure 3A, which shows a cluster analysis of spiking properties of neurons recorded in vitro from slice preparations of the macaque prefrontal cortex, reveals three neurons (of 17 for which data on calcium-binding protein expression was available) in the "FS" cluster that express CB or calretinin, and not PV.

Electrophysiological studies are required to determine whether the PV-ir Kv3.1b-immunonegative neurons exhibit the properties characteristic of FS cells. This capability, if observed, would likely arise through the expression of Kv3 channels comprised entirely of Kv3.2 subunits, as our own preliminary studies indicate that Kv3.3 proteins, the other Kv3 subunits that produce channels with similar electrophysiological properties, are, at best, extremely sparsely expressed in macaque V1. Electrophysiological experiments are also required to ascertain the spiking properties of the CB-ir Kv3-expressing interneuron population.

In layers 5 and 6 of the rodent neocortex, about 27% of Kv3.2-ir neurons (but not Kv3.1b-ir neurons) strongly express the calcium-binding protein CB (Chow et al., 1999). Chow et al. (1999) used triple labeling to show that most of these neurons express somatostatin and are to be likely an independent population from those expressing PV. The electrophysiological properties of these cells remain to be studied, but these cells may include the somatostatin-containing FS-like X-94 interneurons recently described by Ma et al. (2006). Therefore, in the rodent neocortex, Kv3.2 subunits do appear to be expressed in a proportion of CB-ir cells that are not classical FS cells but may share some properties with these neurons.

In macaque V1, the proportion of Kv3.1b-ir neurons that is GABAergic (≈75%) is roughly equal to the proportion that is PV-ir. The same is true for Kv3.2-ir neurons. This makes it difficult, on initial inspection, to interpret the population of Kv3 subunit-immunoreactive neurons that express CB but not PV as a population of GABAergic interneurons, and yet it has been demonstrated previously that darkly stained CB-ir neurons in macaque V1 are GABAergic (Van Brederode et al., 1990). There are three possible explanations for this apparent conflict. First, perhaps all of the Kv3-ir (i.e., Kv3.1b-ir and/or Kv3.2-ir) neurons that are CB-ir also express PV. According to this interpretation, in contrast to findings in the rodent neocortex, in macaque V1 Kv3.2 is not expressed in a distinct population of CB-ir/PV-immunonegative interneurons in layers 5 and 6. This is very unlikely because, as mentioned above, cells expressing both CB and PV are extremely rare in macaque V1 and have only been reported in layers 2 and 3 (Van Brederode et al., 1990). Our CB-ir, Kv3-expressing cells are found in all layers. Alternatively, it might be concluded that some of the PV-ir neurons expressing Kv3 subunits are not GABAergic. Van Brederode et al. (1990) do report that ≈4% of the PV-ir neurons they encountered in macaque V1 appeared not to be GABA-ir. However, the authors also point out that in many cases the PV immunostaining was so dark that it could have obscured the staining for GABA. If these apparently singly labeled neurons do represent a small population of PV-ir neurons that are non-GABAergic, then it is possible that the Kv3 subunits are expressed in GABAergic interneurons that express PV, GABAergic interneurons that express CB (and not PV), and putatively excitatory cells, a small proportion of which express PV. Finally, it is possible that the number of Kv3-ir neurons that express CB falls within the error of the estimates of the Kv3-ir GABAergic population. For example, the proportion of Kv3.2-ir neurons that express GABA in layers 1–4 (76.46 ± 13.32) and layers 5 and 6 (77.51 ± 7.31) may in fact include the population of Kv3.2-ir neurons that express CB, within error. According to this final (and, given the small size of the CB/Kv3 dual-labeled populations, most likely) interpretation, the Kv3.2-ir neurons that express PV and CB may represent nonoverlapping populations of GABAergic interneurons. These questions motivate triple-labeling experiments to precisely determine the degree of overlap between the Kv3-ir populations that express PV and CB.

Differences in the cortical circuit across species

Models of the cortical circuits underlying visual processing provide a theoretical framework for interpreting experimental findings. Additionally, these models may be applicable to understanding the neural mechanisms of sensory processing in general. Finally, such models are directly relevant to experiments that use visual tasks to investigate higher cognitive functions, including reward and motivation, attention, and memory. Although models of visual cortical function are, for historical reasons, based primarily on data collected from cats and primates (Douglas and Martin, 2004), the advent of powerful genetic techniques has led to an increase in the use of rodent models. It is therefore important to characterize and understand where differences in visual cortical anatomy and physiology exist between rodents and other mammals, as these differences need to inform models of visual systems across species.

We have found that there are many similarities between rodents and macaques in the types and distributions of cells that express Kv3 channels. Specifically, in both species, Kv3.1b and Kv3.2 are usually expressed in GABAergic interneurons that express PV, and occasionally also in interneurons that express CB. However, there are marked quantitative differences in the proportions of cell types coexpressing Kv3 channels across species, such as a remarkably larger population of neurons expressing the Kv3 channels in macaque neocortex. There are also qualitative differences, notably the population of the neurons expressing Kv3 that are non-GABAergic.

The cortical circuit, in terms of neuronal types and patterns of intrinsic activity, is widely believed to be canonical across species (Douglas and Martin, 2004). Species differences, when they occur, are often observed within the inhibitory neuronal population (DeFelipe, 1993; DeFelipe et al., 2002).

For example, in prefrontal rodent and primate cortex, anatomically similar neurogliaform inhibitory interneurons show quite distinct functional properties (Povysheva et al., 2007), suggesting that morphological cell types may express the channels responsible for spiking behavior differently, depending on the species. The lack of reports of differences within the excitatory population may be due to the relative paucity of cellular labels that distinguish different classes of excitatory neurons. We report evidence for a class of excitatory cells that express Kv3 channels, which are not observed in the rodent neocortex. These cells may constitute a case of species-dependent variability within the excitatory cell population. Therefore, our findings motivate future in vitro and in vivo electrophysiology studies that would aim to precisely characterize the properties and distributions of neuronal types in the macaque neocortex, specifically of Kv3-expressing neurons, some of which may represent both inhibitory (specifically CB-ir/PV-immunonegative) and excitatory populations that have not been observed in the rodent neocortex.

ACKNOWLEDGMENTS

The authors thank J.A. Movhson, Y. El-Shamayleh, R. Kumbhani, C. Farb, C. Aoki, and M. Schiff for technical assistance, advice, and support.

LITERATURE CITED

Adams I, Brauer K, Arelin C, Hartig W, Fine A, Mader M, Arendt T, Bruckner G. 2001. Perineuronal nets in the rhesus monkey and human basal forebrain including basal ganglia. Neuroscience 108:285–298.

Beaulieu C, Kisvarday Z, Somogyi P, Cynader M, Cowey A. 1992. Quantitative distribution of GABA-immunopositive and -immunonegative neurons and synapses in the monkey striate cortex (area 17). Cereb Cortex 2:295–309.

Benson DL, Isackson PJ, Gall CM, Jones EG. 1992. Contrasting patterns in the localization of glutamic acid decarboxylase and Ca2+/calmodulin protein kinase gene expression in the rat central nervous system. Neuroscience 46:825–849.

Brumberg JC, Nowak LG, McCormick DA. 2000. Ionic mechanisms underlying repetitive high-frequency burst firing in supragranular cortical neurons. J Neurosci 20:4829–4843.

Carder RK, Hendry SHC. 1994. Neuronal characterization, compartmental distribution, and activity-dependent regulation of glutamate immunoreactivity in adult monkey striate cortex. J Neurosci 14:242–262.

Cardin JA, Palmer LA, Contreras D. 2005. Stimulus-dependent gamma (30-50 Hz) oscillations in simple and complex fast rhythmic bursting cells in primary visual cortex. J Neurosci 25:5339–5350.

Cauli B, Audinat E, Lambolez B, Angulo MC, Ropert N, Tsuzuki K, Hestrin S, Rossier J. 1997. Molecular and physiological diversity of cortical nonpyramidal cells. J Neurosci 17:3894–3906.

Celio MR. 1993. Perineuronal nets of extracellular matrix around parvalbumin-containing neurons of the hippocampus. Hippocampus 3:55–60.

Chow A, Erisir A, Farb C, Nadal MS, Ozaita A, Lau D, Welker E, Rudy B. 1999. K^+ channel expression distinguishes subpopulations of parvalbumin- and somatostatin-containing neocortical interneurons. J Neurosci 19:9332–9345.

Condé F, Lund JS, Jacobowitz DM, Baimbridge KG, Lewis DA. 1994. Local circuit neurons immunoreactive for calretinin, calbindin D-28k or parvalbumin in monkey prefrontal cortex: distribution and morphology. J Comp Neurol 341:95–116.

DeFelipe J. 1993. Neocortical neuronal diversity: chemical heterogeneity revealed by colocalization studies of classic neurotransmitters, neuropeptides, calcium-binding proteins, and cell surface molecules. Cereb Cortex 3:273–289.

DeFelipe J, González-Albo MC, Del Río MR, Elston GN. 1999. Distribution and patterns of connectivity of interneuron's containing calbindin, calretinin, and parvalbumin in visual areas of the occipital and temporal lobes of the macaque monkey. J Comp Neurol 412:515–526.

DeFelipe J, Alonso-Nanclares L, Arellano JI. 2002. Microstructure of the neocortex: comparative aspects. J Neurocytol 31:299–316.

Disney AA, Aoki C. 2008. Muscarinic acetylcholine receptors in macaque V1 are most frequently expressed by parvalbumin-immunoreactive neurons. J Comp Neurol 507:1748–1762.

Douglas RJ, Martin KA. 2004. Neuronal circuits of the neocortex. Annu Rev Neurosci 27:419–451.

Elezgarai I, Diez J, Puente N, Azkue JJ, Benitez R, Bilbao A, Knopfel T, Donate-Oliver F, Grandes P. 2003. Subcellular localization of the voltage-dependent potassium channels Kv3.1b in postnatal and adult rat medial nucleus of the trapezoid body. Neuroscience 118:889–898.

Erisir A, Lau D, Rudy B, Leonard CS. 1999. Function of specific K(+) channels in sustained high-frequency firing of fast-spiking neocortical interneurons. J Neurophysiol 82:2476–2489.

Gonchar Y, Burkhalter A. 1997. Three distinct families of GABAergic neurons in rat visual cortex. Cereb Cortex 7:347–358.

Gray CM, McCormick DA. 1996. Chattering cells: superficial pyramidal neurons contributing to the generation of synchronous oscillations in the visual cortex. Science 274:109–113.

Guillery RW. 2002. On counting and counting errors. J Comp Neurol 447:1–7.

Hartig W, Derouiche A, Welt K, Brauer K, Grosche J, Mader M, Reichenbach A, Bruckner G. 1999. Cortical neurons immunoreactive for the potassium channel Kv3.1b subunit are predominantly surrounded by perineuronal nets presumed as a buffering system for cations. Brain Res 842:15–29.

Hendrickson AE, Tillakaratne, NJK, Metha RD, Esclapez M, Erickson A, Vician L, Tobin, AJ. 1994. Differential localization of two glutamic acid decarboxylases (GAD65 and GAD67) in adult monkey visual cortex. J Comp Neurol 343:566–581.

Hendry SHC, Schwark HD, Jones EG, Yan J. 1987. Numbers and proportions of GABA-immunoreactive neurons in different areas of monkey cerebral cortex. J Neurosci 7:1503–1519.

Ho CS, Grange RW, Joho RH. 1997. Pleiotropic effects of a disrupted K+ channel gene: reduced body weight, impaired motor skill and muscle contraction, but no seizures. Proc Natl Acad Sci U S A 94:1533–1538.

Hsu SM, Raine L, Fanger H. 1981. Use of avidin-biotin-peroxidase complex (ABC) immunoperoxidase techniques: a comparison between ABC and unlabeled antibody (PAP) procedures. J Histochem Cytochem 29:577–580.

Ichinohe N, Watakabe A, Miyashita T, Yamamori T, Hashikawa T, Rockland KS. 2004. A voltage-gated potassium channel, Kv3.1b, is expressed by a subpopulation of large pyramidal neurons in layer 5 of the macaque monkey cortex. Neuroscience 129:179–185.

Jones EG, Huntley GW, Benson DL. 1994. Alpha calcium/calmodulin-dependent protein kinase II selectively expressed in a subpopulation of excitatory neurons in monkey sensory-motor cortex: comparison with GAD-67 expression. J Neurosci 14:611–629.

Joshi S, Hawken MJ. 2006. Loose-patch-juxtacellular recording in vivo—a method for functional characterization and labeling of neurons in macaque V1. J Neurosci Methods 156:37–49.

Kaczmarek LK, Bhattacharjee A, Desai R, Gan L, Song P, von Hehn CA, Whim MD, Yang B. 2005. Regulation of the timing of MNTB neurons by short-term and long-term modulation of potassium channels. Hear Res 206:133–145.

Kawaguchi Y, Kubota Y. 1993. Correlation of physiological subgroupings of nonpyramidal cells with parvalbumin- and calbindin$_{D28k}$-immunoreactive neurons in layer V of rat frontal cortex. J Neurophysiol 70:387–396.

Kawaguchi Y, Kubota Y. 1997. GABAergic cell subtype and their synaptic connections in rat frontal cortex. Cereb Cortex 7:478–486.

Lau D, Vega-Saenz de Miera E, Contreras D, Ozaita A, Harvey M, Chow A, Noebels JL, Paylor R, Morgan JI, Leonard CS, Ruby B. 2000. Impaired fast-spiking, suppressed cortical inhibition, and increased susceptibility to seizures in mice lacking Kv3.2 K+ channel proteins. J Neurosci 20:9071–9085.

Li W, Kaczmarek LK, Perney TM. 2001. Localization of two high-threshold potassium channel subunits in the rat central auditory system. J Comp Neurol 437:196–218.

Liu XB, Jones EG. 1996. Localization of alpha type II calcium calmodulin-dependent protein kinase at glutamatergic but not gamma-aminobutyric acid (GABAergic) synapses in thalamus and cerebral cortex. Proc Natl Acad Sci U S A 93:7332–7336.

Lund JS. 1973. Organization of neurons in the visual cortex, area 17, of the monkey (Macaca mulatta). J Comp Neurol 147:455–495.

Ma Y, Hu H, Berrebi AS, Mathers PH, Agmon A. 2006. Distinct subtypes of

somatostatin-containing neocortical interneurons revealed in transgenic mice. J Neurosci 26:5069–5082.

Majlof L, Forsgren PO. 1993. Confocal microscopy: Important considerations for accurate imaging. Methods Cell Biol 38:79–95.

McCormick DA, Connors BW, Lighthall JW, Prince DA. 1985. Comparative electrophysiology of pyramidal and sparsely spiny stellate neurons of the neocortex. J Neurophysiol 54:782–806.

Miles R, Tóth K, Gulyás AI, Hájos N, Freund TF. 1996. Differences between somatic and dendritic inhibition in the hippocampus. Neuron 16:815–823.

Morris NP, Henderson Z. 2000. Perineuronal nets ensheath fast spiking, parvalbumin-immunoreactive neurons in the medial septum/diagonal band complex. Eur J Neurosci 12:828–838.

Mouton PR. 2002. Principles and practices of unbiased stereology: an introduction for bioscientists. Baltimore: Johns Hopkins University Press.

Nowak LG, Azouz R, Sanchez-Vives MV, Gray CM, McCormick DA. 2003. Electrophysiological classes of cat primary visual cortical neurons in vivo as revealed by quantitative analyses. J Neurophysiol 89:1541–1566.

Perney TM, Kaczmarek LK. 1997. Localization of a high threshold potassium channel in the rat cochlear nucleus. J Comp Neurol 386:178–202.

Perney TM, Marshall J, Martin KA, Hockfield S, Kaczmarek LK. 1992. Expression of the mRNAs for the Kv3.1 potassium channel gene in the adult and developing rat brain. J Neurophysiol 68:756–766.

Platt ML, Glimcher PW. 1997. Responses of intraparietal neurons to saccadic targets and visual distractors. J Neurophysiol 78:1574–1589.

Povysheva NV, Zaitsev AV, Kroner S, Krimer OA, Rotaru DC, Gonzalez-Burgos G, Lewis DA, Krimer LS. 2007. Electrophysiological differences between neurogliaform cells from monkey and rat prefrontal cortex. J Neurophysiol 97:1030–1039.

Rajendra S, Lynch JW, Schofield PR. 1997. The glycine receptor. Pharmacol Ther 73:121–146.

Rockland KS, Lund JS. 1983. Intrinsic laminar lattice connections in primate visual cortex. J Comp Neurol 216:303–318.

Rudy B, McBain CJ. 2001. Kv3 channels: voltage-gated K+ channels designed for high-frequency repetitive firing. Trends Neurosci 24:517–526.

Rudy B, Chow A, Lau D, Amarillo YAO, Saganich M, Moreno H, Hernandez-Pineda R, Hernandez-Cruz A, MacIntosh P, Erisir A, Leonard CS, Vega-Saenz de Meira E. 1999. Contributions of Kv3 channels to neuronal excitability. Ann N Y Acad Sci 868:304–343.

Saganich MJ, Vega-Saenz de Miera E, Nadal MS, Baker H, Coetzee WA, Rudy B. 1999. Cloning of components of a novel subthreshold-activating K(+) channel with a unique pattern of expression in the cerebral cortex. J Neurosci 19:10789–10802.

Saganich MJ, Machado E, Rudy B. 2001. Differential expression of genes encoding subthreshold-operating voltage-gated K^+ channels in brain. J Neurosci 21:4609–4624.

Schwartz ML, Zheng DS, Goldman-Rakic PS. 1988. Periodicity of GABA-containing cells in primate prefrontal cortex. J Neurosci 8:1962–1970.

Sekirnjak C, Martone ME, Weiser M, Deerinck T, Bueno E, Rudy B, Ellisman M. 1997. Subcellular localization of the K^+ channel subunit Kv3.1b in selected rat CNS neurons. Brain Res 766:173–187.

Skoglund TS, Pascher R, Berthold C-H. 1996. Aspects of the quantitative analysis of neurons in the cerebral cortex. J Neurosci Methods 70:201–210.

Solomon SG, Peirce JW, Lennie P. 2004. The impact of suppressive surrounds on chromatic properties of cortical neurons. J Neurosci 24:148–160.

Steriade M. 2004. Neocortical cell classes are flexible entities. Nat Rev Neurosci 5:121–134.

Sterio DC. 1984. The unbiased estimation of number and size of arbitrary particles using the disector. J Microsc 134:127–136.

Toledo-Rodriguez M, Blumenfeld B, Wu C, Luo J, Attali B, Goodman P, Markram H. 2004. Correlation maps allow neuronal electrical properties to be predicted from single-cell gene expression profiles in rat neocortex. Cereb Cortex 14:1310–1327.

Van Brederode JFM, Mulligan KA, Hendrickson AE. 1990. Calcium-binding proteins as markers for subpopulations of GABAergic neurons in monkey striate cortex. J Comp Neurol 298:1–22.

Vogt Weisenhorn DM, Illing R-B, Spatz WB. 1995. Morphology and connections of neurons in area 17 projecting to the extrastriate areas MT and 19DM and to the superior colliculus in the monkey Callithrix jacchus. J Comp Neurol 362:233–255.

von Hehn CA, Bhattacharjee A, Kaczmarek LK. 2004. Loss of Kv3.1 tonotopicity and alterations in cAMP response element-binding protein signaling in central auditory neurons of hearing impaired mice. J Neurosci 24:1936–1940.

Wang LY, Gan L, Forsythe ID, Kaczmarek LK. 1998. Contribution of the Kv3.1 potassium channel to high-frequency firing in mouse auditory neurons. J Physiol (Lond) 509:183–194.

Weiser M, Vega-Saenz de Miera E, Kentros C, Moreno H, Franzen L, Hillman D, Baker H, Rudy B. 1994. Differential expression of Shaw-related K^+ channels in the rat central nervous systems. J Neurosci 14:949.

Weiser M, Bueno E, Sekirnjak C, Martone ME, Baker H, Hillman D, Chen S, Thornhill W, Ellisman M, Rudy B. 1995. The potassium channel subunit Kv3.1b is localized to somatic and axonal membranes of specific populations of CNS neurons. J Neurosci 15:4298–4314.

Wong-Riley M. 1979. Changes in the visual system of monocularly sutured or enucleated cats demonstrable with cytochrome oxidase histochemistry. Brain Res 171:11–28.

Wouterlood FG, Jorritsma-Byham B. 1993. The anterograde neuroanatomical tracer biotinylated dextran-amine: comparison with the tracers *Phaseolus vulgaris*-leucoagglutinin in preparations for electron microscopy. J Neurosci Methods 48:75–87.

Zaitsev AV, Gonzalez-Burgos G, Povysheva NV, Kroner S, Lewis DA, Krimer LS. 2005. Localization of calcium-binding proteins in physiologically and morphologically characterized interneurons of monkey dorsolateral prefrontal cortex. Cereb Cortex 15:1178–1186.